Fast and well-conditioned boundary integral equation solvers for the numerical simulation of graphene plasmon

by

Yu Chen

A dissertation submitted to the Graduate Faculty of
Auburn University
in partial fulfillment of the
requirements for the Degree of
Doctor of Philosophy

Auburn, Alabama
August 4, 2018

Keywords: graphene plasmon, boundary integral equation, Nystrom method

Approved by

Yanzhao Cao, Chair, Professor of Mathematics and Statistics
Dmitry Glotov, Associate Professor of Mathematics and Statistics
Wenxian Shen,Professor of Mathematics and Statistics
Richard Zalik, Professor of Mathematics and Statistics

Abstract

Surface plasmonic polaritons (SPPs) are evanescent electromagnetic waves coupled to free electron plasma oscillations. It was first observed in metallic gratings in 1902 by Wood [57]. Modern plasmonics gained renewed interest since the discovery of the extraordinary optical transmission through a periodic array of subwavelength hole arrays [15]. The strong confinement of SPPs in the subwavelength scales and their huge electromagnetic field enhancements have led to significant applications of plasmonics structures in near-field imaging, spectroscopy and bio-sensing, solar cells, nano-photonics, etc. Graphene is rapidly emerging as a powerful plasmonic material recently by combining the appealing features of SPPs and easiness to tune electrically. It also opens applications of SPPs in lower frequency regimes such as the terahertz to mid-infrared frequencies [1, 6, 11, 18, 20, 34, 35, 58].

This thesis is concerned with computational modeling of plasmonic phenomenon in graphene. Two main difficulties arise in solving the associated mathematical models numerically. First, surface plasmonic modes are strongly confined with subwavelength scales, and at the same time, they are highly oscillatory along the graphene surface. Hence numerical schemes have to be designed so as to resolve the oscillatory nature of plasmonic waves. Second, the two-dimensional graphene has sharp edges. Such edge effect may give rise to additional difficulties, such as ill-conditioning of the discretized linear system.

In this thesis, we develop an integral-equation solver for numerical simulations of graphene plasmon. The integral equation is formulated along the graphene surface, which reduces the degree of freedom significantly compared with volumetric methods. Another advantage is that the radiation condition at infinity is enforced automatically. Due to the edge effect mentioned above, the classical Calderon formula does not lead to a well-conditioned integral formulation anymore. To alleviate the ill-conditioning, following the ideas in [8], we regularize the integral equation using scaled integral operators and generalized Calderon formula. The Nystrom

scheme is then applied to discretize the integral operators and the Generalized minimal residual (GMRES) iterative method is employed to solve the linear system. Numerical examples are demonstrated to illustrate the effectiveness of the proposed integral-equation solver. Finally, we carry out numerical analysis to study the errors arising in numerical approximation of the integral equation and its solution.

Acknowledgments

I would like to express my deepest gratitude to my major Professor Yanzhao Cao for his encouragement, guidance and help all the time. In Spring 2013, with Prof. Cao's strong encouragement, I made the last-minute decision to transfer to the Ph.D. program in Auburn University. He gave me a big help through the application process. His enthusiasm for mathematics and dieligence have been inspiring me over the years. Every time when I met difficulties on the research project, it was him who told me firmly that I can do it; it was him who guided me with patience on every meeting and presentation.

I would like to thank Professors Dmitry Glotov, Wenxian Shen and Richard Zalik for being on my committee and valuable suggestions. I also would like to thank Professor Yu Lin from Department of Physics for being the university reader. I am grateful to Professors Tin-Yau Tam, Ulrich Albrecht and Xiaoying Han as well as the staff in Department of Mathematics and Statistics for their help.

My special thanks go to Professors Zhengfang Zhou, Tien-Yien Li and Jeffrey Schenker in Michigan State University. Prof. Zhou offered me a ton of help even before I began my Ph.D. study in Michigan State University in Fall 2010. Profs. Li and Schenker built my confidence when I took their classes. It really means a lot to me as a fresh Ph.D. student. I appreciate their strong support when I finally decided to transfer to Auburn University due to family reason.

I would like to thank Liangmin and Liping for being great friends, for discussing math problems together, for sharing ups and downs. I would also thank Jing, my best friend since teenage years. Her tough Ph.D. life always motivates me and reminds me that how lucky I am to work with Prof. Cao.

My deepest appreciation goes to my family. I own a debt of thanks to my husband, Junshan Lin, for the strong encouragement and for supporting the family. I am so grateful to my parents for being dedicated and supportive in all stages of my life; for all the sacrifice they made since

I decided to quit my job and came to the United States in 2009. I would also thank my parents in-law for their support and understanding all the time.

Table of Contents

List of Figures

List of Tables

Chapter 1

Introduction

1.1 Background on graphene plasmon

Plasmons, which are collective oscillations of electrons in conducting materials, possess a number of appealing properties for photonic technologies. The surface plasmonic polaritons (SPPs) phenomenon was first observed and investigated in metallic gratings in 1902 by Wood (cf. [57]). This is so-called Wood anomaly. Theoretical explanation for the origin of the Wood anomaly began with Rayleigh in 1907 (cf. [49]). But not until 1937 it was fully understood that surface plasmonic resonances give rise to such anomaly (cf. [16, 17]).

It was the discovery of the extraordinary optical transmission through a periodic array of subwavelength hole arrays by T. Ebbesen in 1998 (cf. [15]) that sparked new interest in plasmonics. Since then tremendous efforts has been devoted to the investigation and application of plasmonics in physics and engineering (see [1, 20, 42] and references therein for an overview). The small spatial extension of SPPs compared with the light wavelength has been exploited to achieve super-resolution for optical imaging. The huge electromagnetic field enhancement produced by the strong interaction with the conducting material is also used in bio-sensing, such as surface-enhanced Raman scattering (SERS) techniques, and other nano-optics techniques, such as solar cells, nano-photonics, etc[19, 27, 39].

Graphene, a two-dimensional, hexagonal lattice consisting of a single atomic layer of carbon atoms (cf. Figure 1.1) , has recently emerged as a powerful plasmonic material. It combines the appealing features above with the ability of being electrically tunable. In addition, it has

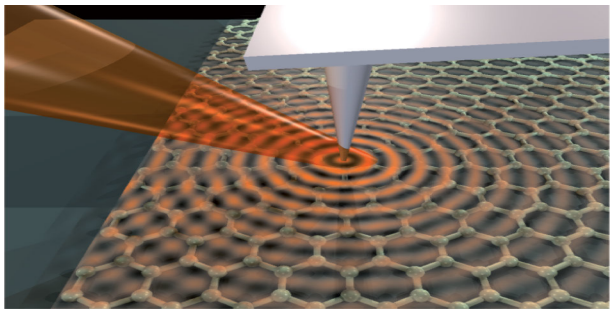

Figure 1.1: A schematic plot of graphene plasmon.

been shown that the plasmon wave vector is two orders larger than the free space wave vector, which translates to the stronger confinement than the metallic plasmons. Very importantly, the graphene plasmon also opens new applications in the terahertz to mid-infrared regime, for which its plasmonic resonance resides. The plasmon in this frequency regime is much less explored than in the visible-light regime. We refer to [2, 6, 11, 18, 20, 34, 35, 58] for a complete overview of the theoretical investigation as well as experimental studies on graphene plasmon.

1.2 Mathematical model

In this section, we introduce the mathematical model for the electromagnetic wave scattering by graphene sheet. This will be used throughout the rest of the thesis.

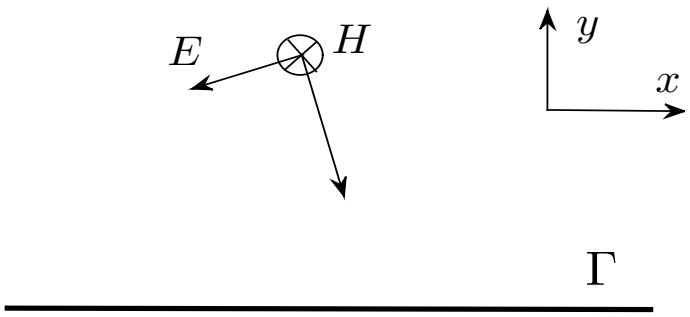

Figure 1.2: Geometry of the problem.

Consider a time-harmonic (with $e^{-i\omega t}$ time dependence) plane wave $(\mathbf{E}^i, \mathbf{H}^i)$ that impinges on the graphene sheet sitting in the vacuum. The graphene layer is infinite and invariant along z direction. Let us denote its cross-section by Γ (see Figure 1.2). Here Γ is a finite open curve

in $\mathbb{R}^2$. The total field $(\mathbf{E}, \mathbf{H})$ after the scattering consists of the incident wave $(\mathbf{E}^i, \mathbf{H}^i)$ and the scattered wave $(\mathbf{E}^s, \mathbf{H}^s)$. The electromagnetic field $(\mathbf{E}, \mathbf{H})$ is governed by the time-harmonic Maxwell's equations in the vacuum (cf. [23]):

$$\begin{cases} \nabla \times \mathbf{E} = i\omega\mu_0 \mathbf{H}, \\ \nabla \cdot \mathbf{E} = 0, \\ \nabla \times \mathbf{H} = -i\omega\varepsilon_0 \mathbf{E}, \\ \nabla \cdot \mathbf{H} = 0. \end{cases} \tag{1.1}$$

Here ω is the angular frequency, ε_0 and μ_0 are permittivity and permeability respectively.

Along the graphene interface Γ, the electromagnetic field satisfies the following continuity conditions:

$$\nu \times (\mathbf{E}_+ - \mathbf{E}_-) = 0, \qquad \nu \times (\mathbf{H}_+ - \mathbf{H}_-) = J_s, \tag{1.2}$$

$$\nu \cdot (\varepsilon_0 \mathbf{E}_+ - \varepsilon_0 \mathbf{E}_-) = \rho_s, \qquad \nu \cdot (\mu_0 \mathbf{H}_+ - \mu_0 \mathbf{H}_-) = 0. \tag{1.3}$$

Here $\mathbf{E}_\pm$ and $\mathbf{H}_\pm$ denote the electric and magnetic fields above and below the graphene, respectively, ν denotes the unit normal vector along the interface Γ, J_s and ρ_s are surface current density and charge density respectively. In addition, at infinity the scattered field satisfies the Silver-Muller radiation condition:

$$\lim_{|x|\to\infty} (\sqrt{\mu_0}\, \mathbf{H}^s \times x - |x| \cdot \sqrt{\varepsilon_0}\, \mathbf{E}^s) = 0. \tag{1.4}$$

(1.2) implies that the tangential components of the electric field is continuous across the graphene sheet, while the tangential components of the magnetic field is discontinuous across the graphene sheet and the jump is given by the surface current density J_s. By Ohm's law, the surface current density equals the product of the conductivity and the electric current. Condition (1.2) implies that the jump for the normal components of the electric field across the graphene sheet is given by the surface charge density ρ_s. In our model, the plane wave is generated by sources located at infinity, and consequently $\rho_s = 0$.

In this thesis, we consider the transverse magnetic (TM) polarization by assuming that the magnetic field is pointing along the z direction. That is, the magnetic field $\mathbf{H} = (0, 0, u)$. Correspondingly, the incident wave $\mathbf{H}^i = (0, 0, u^i)$, where $u^i = e^{ik(\alpha x+\beta y)}$ is a plane wave. Since graphene is infinite and invariant along the z direction, u is the function of x and y only.

From $\nabla \times \mathbf{H} = -i\omega\varepsilon_0\mathbf{E}$ and $\nabla \times \mathbf{E} = i\omega\mu_0\mathbf{H}$ in (1.1), it follows that

$$\nabla \times (\nabla \times \mathbf{H}) = -i\omega\varepsilon_0 (\nabla \times \mathbf{E}) = \omega^2\varepsilon_0\mu_0(0, 0, u).$$

A direct computation of $\nabla \times (\nabla \times \mathbf{H})$ using $\mathbf{H} = (0, 0, u)$ yields that

$$\nabla \times (\nabla \times \mathbf{H}) = (0, 0, -\Delta u).$$

Therefore, u satisfies the Helmhotlz equation in $\mathbb{R}^2\backslash\Gamma$,

$$\Delta u + k^2 u = 0,$$

where $k = \omega\sqrt{\varepsilon_0\mu_0}$ is the wavenumber.

From the continuity condition $\nu \times (\mathbf{E}_+ - \mathbf{E}_-) = 0$ in (1.2) and using the relation $\nabla \times \mathbf{H} = -i\omega\varepsilon_0\mathbf{E}$, it can be shown that

$$\begin{aligned} & \nu \times ((\nabla \times \mathbf{H})_+ - (\nabla \times \mathbf{H})_-) \\ = \; & \left(0, 0, \left(\frac{\partial u}{\partial \nu}\right)_+ - \left(\frac{\partial u}{\partial \nu}\right)_-\right) \\ = \; & 0. \end{aligned}$$

Therefore, we obtain the following condition along the interface Γ,

$$\left(\frac{\partial u}{\partial \nu}\right)_+ = \left(\frac{\partial u}{\partial \nu}\right)_- \quad \text{on } \Gamma.$$

On the other hand, by a combination of the continuity condition and the Ohm's Law, it follows that

$$\nu \times (\mathbf{H}_+ - \mathbf{H}_-) = J_s = \sigma \mathbf{E}_t = \sigma \cdot \nu \times (\mathbf{E} \times \nu).$$

An explicit calculation using $\mathbf{H} = (0, 0, u)$ implies that

$$u_+ - u_- = \frac{i\sigma}{\omega \varepsilon_0} \frac{\partial u}{\partial \nu} = \frac{i\sigma}{k} \sqrt{\frac{\mu_0}{\varepsilon_0}} \frac{\partial u}{\partial \nu} \quad \text{on } \Gamma.$$

Therefore, the Maxwell's equations can be reduced to the following model in the xy-plane:

$$\begin{cases} \Delta u + k^2 u = 0 & \text{in } \mathbb{R}^2 \backslash \Gamma, \\ \left(\dfrac{\partial u}{\partial \nu} \right)_+ = \left(\dfrac{\partial u}{\partial \nu} \right)_- & \text{on } \Gamma, \\ u_+ - u_- = \dfrac{i\sigma}{k} \sqrt{\dfrac{\mu_0}{\varepsilon_0}} \dfrac{\partial u}{\partial \nu} & \text{on } \Gamma. \end{cases} \tag{1.5}$$

Here c is the speed of light, $k = \omega/c$ is the wavenumber, σ is the conductivity of the graphene depending on the frequency ω. In the long-wavelength regime, it can be described by the Drude model (cf. [34, 35]):

$$\sigma(\omega) = \frac{ie^2 |E_F|}{\pi \hbar^2 (\omega + i/\tau_e)},$$

where e is the electronic charge, $\hbar$ is the reduced Planck constant, E_F is the chemical potential, and τ_e is the momentum relaxation time. In addition, the scattered field u^s, which is given by $u - u^i$, satisfies the Sommerfeld radiation condition

$$\lim_{|x| \to \infty} \sqrt{r} \left(\frac{\partial u^s}{\partial r} - iku^s \right) = 0. \tag{1.6}$$

1.3 Existing methods for solving the scattering problem along graphene sheet

If the graphene sheet is flat and infinite such that it occupies the whole xy-plane or it is semi-infinite, then analytical expressions for the electromagnetic field are available [40, 41]. The finite element method (FEM) has been applied to the model in such instances numerically [36]. When the graphene sheet is finite, then a numerical method has to be employed to solve

the scattering problem. In this regard, a finite element solver has been developed and implemented [37]. We also refer to a surface perturbation approach for solving the problem when the graphene is periodic in one direction [44].

Current modeling algorithms such as the finite element method are extremely costly even for the two-dimensional model, and the extension to the three-dimensional model would require even more computational resources. The high cost for the finite element method is attributed to two reasons. First, FEM relies on the discretization in the domain where the graphene sits, hence the perfect matched layer (PML) or other radiation conditions have to be applied to truncate the infinite domain to a finite one (Figure 1.3). Second, due to the strong localization of the graphene plasmon waves and their highly oscillatory nature near the graphene surface, the mesh has to be extremely refined to capture the physical phenomenon (See Figure 1.4).

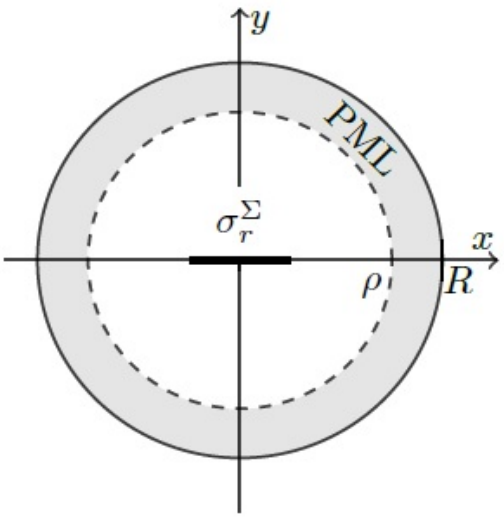

Figure 1.3: The PML layer is applied to truncate the infinite domain into a finite one (after [37]).

In this thesis, we aim to develop an efficient and accurate integral-equation method for computational modeling of graphene plasmons. The integral equation is set up along the graphene surface, which reduces the degree of freedom significantly compared with the finite element methods. In addition, the radiation condition at infinity is enforced automatically in the integral formulation and no artificial radiation condition needs to be imposed. We also

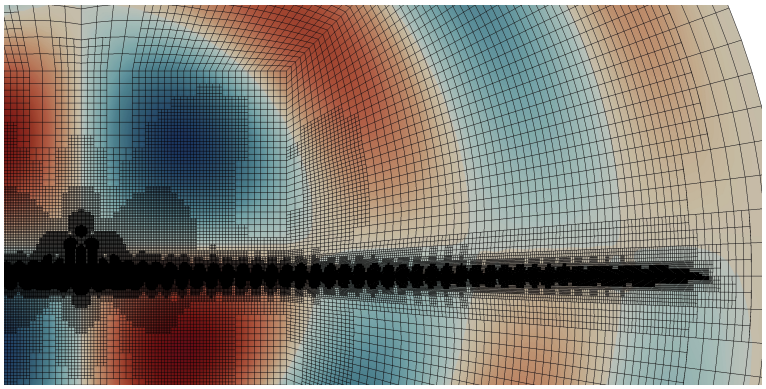

Figure 1.4: Finite element mesh used in the simulation of graphene plasmon (after [38]).

apply high-order Nystrom scheme to discretize the integral operators and employ the Calderon formula technique in order to alleviate the ill-conditioning of the integral equation formulation.

Chapter 2

Layer potentials and the Calderon formula

In this chapter, we introduce the layer potentials and collect some main properties for layer potentials. We also introduce the well-known Calderon formula for the integral equations. The readers are referred to [13, 14, 22, 31, 46] for more details.

2.1 Layer potential

Throughout this chapter, we denote D by a bounded domain of class C^2. Let ∂D be its boundary and ν be the unit normal vector on the boundary that is directed into the exterior of D. We introduce single-layer and double-layer potentials:

Definition 2.1

$$u(x) := \int_{\partial D} \Phi(x,y)\phi(y)ds_y, \quad x \in \mathbb{R}^m \backslash \partial D,$$

and

$$v(x) := \int_{\partial D} \frac{\partial \Phi(x,y)}{\partial \nu_y}\phi(y)ds_y, \quad x \in \mathbb{R}^m \backslash \partial D,$$

where ϕ is the density function, $\Phi(x,y)$ is the fundamental solution of Helmholtz equation.

The single-layer potential can be extended continuously throughout $\mathbb{R}^m$, while its derivative attains a jump when crossing the boundary ∂D. These are stated in the following two theorems (cf. [31]).

Theorem 2.1 *Let ∂D be of class C^2 and $\phi \in C(\partial D)$. Then the single-layer potential u with density ϕ is continuous throughout $\mathbb{R}^m$. On the boundary, it satisfies*

$$u(x) = \int_{\partial D} \Phi(x, y)\phi(y)ds_y, \quad x \in \partial D, \tag{2.1}$$

where the integral exists as an improper integral.

Theorem 2.2 *Let ∂D be of class C^2. Then for the single-layer potential u with continuous density ϕ we have*

$$\frac{\partial u_\pm}{\partial \nu}(x) = \int_{\partial D} \frac{\partial \Phi(x, y)}{\partial \nu_x}\phi(y)ds_y \mp \frac{1}{2}\phi(x), \quad x \in \partial D, \tag{2.2}$$

where

$$\frac{\partial u_\pm}{\partial \nu}(x) := \lim_{h \to 0^+} \nu(x) \cdot \nabla u(x \pm h\nu_x)$$

is to be understood in the sense of uniform convergence on ∂D and where the integral exists as an improper integral.

The following two theorems state the properties of the double-layer potential and its derivative when it crosses the boundary ∂D (cf. [31]).

Theorem 2.3 *Let ∂D be of class C^2, the double-layer potential v with continuous density ϕ can be continuously extended from D to $\bar{D}$ and from $\mathbb{R}^m \backslash \bar{D}$ to $\mathbb{R}^m \backslash D$ with limiting values*

$$v_\pm(x) = \int_{\partial D} \frac{\partial \Phi(x, y)}{\partial \nu_y}\phi(y)ds_y \pm \frac{1}{2}\phi(x), \quad x \in \partial D, \tag{2.3}$$

where

$$v_\pm(x) := \lim_{h \to 0^+} v(x \pm h\nu_x) \tag{2.4}$$

and where the integral exists as an improper integral.

Theorem 2.4 *Let ∂D be of class C^2. Then the double-layer potential v with continuous density ϕ satisfies*

$$\lim_{h \to 0^+} \nu_x \cdot \{\nabla v(x + h\nu_x) - \nabla v(x - h\nu_x)\} = 0 \tag{2.5}$$

uniformly for all $x \in \partial D$.

2.2 Calderon formula

In this section, we state the classical Calderon formula on the closed curve ∂D (cf. [14]). Let us introduce the following integral operators.

For $x \in \Gamma$, let

$$
\begin{aligned}
(\tilde{\mathcal{S}}\phi)(x) &:= \int_\Gamma \Phi(x,y)\phi(y)ds_y, && (2.6)\\
(\tilde{\mathcal{K}}\phi)(x) &:= \int_\Gamma \frac{\partial \Phi(x,y)}{\partial \nu_y}\phi(y)ds_y, && (2.7)\\
(\tilde{\mathcal{K}}'\phi)(x) &:= \int_\Gamma \frac{\partial \Phi(x,y)}{\partial \nu_x}\phi(y)ds_y, && (2.8)\\
(\tilde{\mathcal{T}}\phi)(x) &:= \int_\Gamma \frac{\partial^2 \Phi(x,y)}{\partial \nu_x \partial \nu_y}\phi(y)ds_y. && (2.9)
\end{aligned}
$$

We define the Calderon projector as

$$
\mathcal{C} := \begin{pmatrix} \frac{1}{2}\mathcal{I} - \tilde{\mathcal{K}} & \tilde{\mathcal{S}} \\ -\tilde{\mathcal{T}} & \frac{1}{2}\mathcal{I} + \tilde{\mathcal{K}}' \end{pmatrix},
$$

where $\mathcal{I}$ is the identity operator.

Theorem 2.5 *Let D be a bounded domain, the boundary ∂D be a class of C^2. Then $\mathcal{C}$ maps $C^{1+\alpha}(\partial D) \times C^{\alpha}(\partial D)$ into itself continuously. Morever,*

$$
\mathcal{C}^2 = \mathcal{C}.
$$

Consequently, we have the following identities:

$$
\begin{aligned}
\tilde{\mathcal{S}}\tilde{\mathcal{T}} &= -\frac{1}{4}\mathcal{I} + \tilde{\mathcal{K}}^2, && (2.10)\\
\tilde{\mathcal{T}}\tilde{\mathcal{S}} &= -\frac{1}{4}\mathcal{I} + \tilde{\mathcal{K}}'^2, && (2.11)\\
\tilde{\mathcal{K}}\tilde{\mathcal{S}} &= \tilde{\mathcal{S}}\tilde{\mathcal{K}}', && (2.12)
\end{aligned}
$$

$$\tilde{\mathcal{T}}\tilde{\mathcal{K}} \;=\; \tilde{\mathcal{K}}'\tilde{\mathcal{T}}. \tag{2.13}$$

Proof: Let $u(x)$ be the solution to Helmholtz equation and $\Phi(x,y)$ is the fundamental solution to Helmholtz equation. Then by Green's formula, for $x \in \partial D$ and $x - h\nu_x \in D$,

$$u(x-h\nu_x) = \int_{\partial D} \Phi(x-h\nu_x, y)\frac{\partial u(y)}{\partial \nu_y} ds_y - \int_{\partial D} \frac{\partial \Phi(x-h\nu_x, y)}{\partial \nu_y} u(y)\, ds_y. \tag{2.14}$$

Taking the limit as $h \to 0^+$ and by Theorem 2.1 and 2.3, we have

$$u(x) = \int_{\partial D} \Phi(x,y)\frac{\partial u(y)}{\partial \nu_y} ds_y - \left(\int_{\partial D} \frac{\partial \Phi(x,y)}{\partial \nu_y} u(y)\, ds_y - \frac{1}{2}u(x) \right),\ x \in \partial D.$$

which is equivalent to

$$u(x) = \tilde{\mathcal{S}}\frac{\partial u}{\partial \nu}(x) - \tilde{\mathcal{K}}u(x) + \frac{1}{2}u(x). \tag{2.15}$$

For $x - h\nu_x \in D$, take the normal derivative of (2.14) yields to

$$\frac{\partial u(x-h\nu_x)}{\partial \nu_x} = \int_{\partial D} \frac{\partial \Phi(x-h\nu_x, y)}{\partial \nu_x}\frac{\partial u(y)}{\partial \nu_y} ds_y - \int_{\partial D} \frac{\partial^2 \Phi(x-h\nu_x, y)}{\partial \nu_x \partial \nu_y} u(y)\, ds_y.$$

Taking the limit as $h \to 0^+$ and by Theorem 2.2 and 2.4, we have

$$\frac{\partial u}{\partial \nu}(x) = \int_{\partial D} \frac{\partial \Phi(x,y)}{\partial \nu_x}\frac{\partial u(y)}{\partial \nu_y} ds_y + \frac{1}{2}\frac{\partial u}{\partial \nu}(x) - \int_{\partial D} \frac{\partial^2 \Phi(x,y)}{\partial \nu_x \partial \nu_y} u(y)\, ds_y.$$

That is,

$$\frac{\partial u}{\partial \nu}(x) = \tilde{\mathcal{K}}'\frac{\partial u}{\partial \nu}(x) + \frac{1}{2}\frac{\partial u}{\partial \nu}(x) - \tilde{\mathcal{T}}u. \tag{2.16}$$

From (2.15) and (2.16), it is obvious that

$$\begin{pmatrix} u(x) \\ \dfrac{\partial u}{\partial \nu}(x) \end{pmatrix} = \begin{pmatrix} \dfrac{1}{2}\mathcal{I} - \tilde{\mathcal{K}} & \tilde{\mathcal{S}} \\ -\tilde{\mathcal{T}} & \dfrac{1}{2}\mathcal{I} + \tilde{\mathcal{K}}' \end{pmatrix} \begin{pmatrix} u(x) \\ \dfrac{\partial u}{\partial \nu}(x) \end{pmatrix}. \tag{2.17}$$

From (2.17), it is easy to see that $\mathcal{C}$ maps $C^{1+\alpha}(\partial D) \times C^{\alpha}(\partial D)$ into itself and $\mathcal{C}^2 = \mathcal{C}$.

$$\begin{pmatrix} \frac{1}{2}\mathcal{I} - \tilde{\mathcal{K}} & \tilde{\mathcal{S}} \\ -\tilde{\mathcal{T}} & \frac{1}{2}\mathcal{I} + \tilde{\mathcal{K}}' \end{pmatrix} \begin{pmatrix} \frac{1}{2}\mathcal{I} - \tilde{\mathcal{K}} & \tilde{\mathcal{S}} \\ -\tilde{\mathcal{T}} & \frac{1}{2}\mathcal{I} + \tilde{\mathcal{K}}' \end{pmatrix} = \begin{pmatrix} \frac{1}{2}\mathcal{I} - \tilde{\mathcal{K}} & \tilde{\mathcal{S}} \\ -\tilde{\mathcal{T}} & \frac{1}{2}\mathcal{I} + \tilde{\mathcal{K}}' \end{pmatrix}$$

implies that

$$\begin{aligned} \tilde{\mathcal{S}}\tilde{\mathcal{T}} &= -\frac{1}{4}\mathcal{I} + \tilde{\mathcal{K}}^2, \\ \tilde{\mathcal{T}}\tilde{\mathcal{S}} &= -\frac{1}{4}\mathcal{I} + \tilde{\mathcal{K}'}^2, \\ \tilde{\mathcal{K}}\tilde{\mathcal{S}} &= \tilde{\mathcal{S}}\tilde{\mathcal{K}}', \\ \tilde{\mathcal{T}}\tilde{\mathcal{K}} &= \tilde{\mathcal{K}}'\tilde{\mathcal{T}}. \end{aligned}$$

The Calderon formula states that the composition of the unbounded hypersingular operator $\tilde{\mathcal{T}}$ and the single-layer operator $\tilde{\mathcal{S}}$ yields a compact perturbation of the identity, which is a well-posed operator. As such the formula provides a natural regularization strategy for the hypersingular operator $\tilde{\mathcal{T}}$. That is, the single-layer operator $\tilde{\mathcal{S}}$ serves as an effective preconditioner for $\tilde{\mathcal{T}}$ when solving the discretized linear system.

Chapter 3

Well-conditioned boundary integral equation

In this chapter, we set up a well-conditioned boundary integral equation for solving the scattering problem (1.5) - (1.6). In Section 3.1, we deduce the boundary integral formulation. In Section 3.2, we introduce regularization strategy to obtain a well-conditioned boundary integral equation.

3.1 Boundary integral formulation

Let

$$\Phi(x,y) = \frac{i}{4}H_0^{(1)}(k|x-y|)$$

be the fundamental solution to the Helmholtz equation in the free space satisfying that

$$\Delta\Phi(x,y) + k^2\Phi(x,y) = -\delta(x-y).$$

Here $H_0^{(1)}$ is the first kind Hankel function of zero order.

Let Γ be the graphene sheet. As shown in figure 3.1, we choose a curve $\tilde{\Gamma}$ such that $\Gamma \cup \tilde{\Gamma}$ is a closed and smooth curve in $\mathbb{R}^2$. The domain enclosed by $\Gamma \cup \tilde{\Gamma}$ is denoted by D_-. We also choose a sufficiently large disk B_R with radius R such that it includes the domain D_-. The domain enclosed by $\Gamma \cup \tilde{\Gamma}$ and ∂B_R is denoted as D_+.

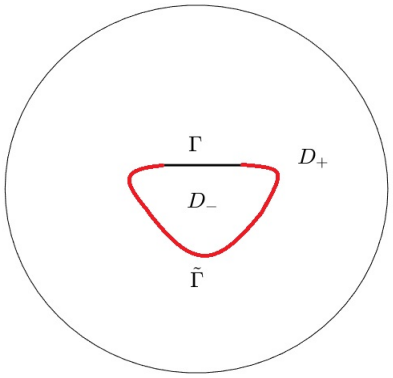

Figure 3.1: Interior and exterior domain D_- and D_+.

By Green's second identity, the scattered field u^s in the exterior and interior domains can be expressed as

$$\begin{aligned} u^s(x) &= \int_{\partial D_-} \frac{\partial \Phi(x,y)}{\partial \nu_y} u^s_+(y) - \Phi(x,y) \left(\frac{\partial u^s}{\partial \nu_y}\right)_+ (y)\, ds_y \\ &\quad + \int_{|y|=R} \Phi(x,y) \frac{\partial u^s(y)}{\partial \nu_y} - \frac{\partial \Phi(x,y)}{\partial \nu_y} u^s(y)\, ds_y \quad x \in D_+; \\ u^s(x) &= \int_{\partial D_-} \Phi(x,y) \left(\frac{\partial u^s}{\partial \nu_y}\right)_- (y) - \frac{\partial \Phi(x,y)}{\partial \nu_y} u^s_-(y)\, ds_y \quad x \in D_-. \end{aligned} \tag{3.1}$$

Here ν is the unit normal vector along Γ directed into D_+. For $h > 0$, $f_+(x)$ and $f_-(x)$ in the above integral are defined as follows:

$$f_+(x) = \lim_{h \to 0^+} f(x + h\nu), \quad x + h\nu \in D_+ \tag{3.2}$$

$$f_-(x) = \lim_{h \to 0^+} f(x - h\nu), \quad x - h\nu \in D_-. \tag{3.3}$$

For the second term of (3.1), that is the integral on the circle with radius R, we have

$$\begin{aligned} &\int_{|y|=R} \Phi(x,y) \frac{\partial u^s(y)}{\partial \nu_y} - \frac{\partial \Phi(x,y)}{\partial \nu_y} u^s(y)\, ds_y \\ = &\int_{|y|=R} \Phi(x,y) \left(\frac{\partial u^s(y)}{\partial \nu_y} - iku^s(y)\right) ds_y - \int_{|y|=R} \left(\frac{\partial \Phi(x,y)}{\partial \nu_y} - ik\Phi(x,y)\right) u^s(y)\, ds_y. \end{aligned}$$

Since both $u^s(y)$ and $\Phi(x,y)$ satisfy the Sommerfeld radiation condition (1.6), thus as $R \to \infty$, the second term of (3.1) vanishes. It follows that

$$u^s(x) = \int_{\partial D_-} \frac{\partial \Phi(x,y)}{\partial \nu_y} u^s_+(y) - \Phi(x,y) \left(\frac{\partial u^s}{\partial \nu_y}\right)_+ (y)\, ds_y \quad x \in D_+; \tag{3.4}$$

$$u^s(x) = \int_{\partial D_-} \Phi(x,y) \left(\frac{\partial u^s}{\partial \nu_y}\right)_- (y) - \frac{\partial \Phi(x,y)}{\partial \nu_y} u^s_-(y)\, ds_y \quad x \in D_-. \tag{3.5}$$

Let $h > 0$. For any $x \in \Gamma \cup \tilde{\Gamma}$, ν_x is the unit normal vector along Γ directed into D_+, so $x + h\nu_x \in D_+$, while $x - h\nu_x \in D_-$. Taking the normal derivative of (3.4) and (3.5) yields

$$\frac{\partial u^s}{\partial \nu_x}(x + h\nu_x) = \int_{\partial D_-} \frac{\partial^2 \Phi(x + h\nu_x, y)}{\partial \nu_x \partial \nu_y} u^s_+(y) - \frac{\partial \Phi(x + h\nu_x, y)}{\partial \nu_x} \left(\frac{\partial u^s}{\partial \nu_y}\right)_+ (y)\, ds_y,$$

$$\frac{\partial u^s}{\partial \nu_x}(x - h\nu_x) = \int_{\partial D_-} \frac{\partial \Phi(x - h\nu_x, y)}{\partial \nu_x} \left(\frac{\partial u^s}{\partial \nu_y}\right)_- (y) - \frac{\partial^2 \Phi(x - h\nu_x, y)}{\partial \nu_x \partial \nu_y} u^s_-(y)\, ds_y.$$

We take the limit $h \to 0^+$ for the above layer potentials. From Theorem 2.4 and Theorem 2.2, we see that

$$\left(\frac{\partial u^s}{\partial \nu_x}\right)_+ (x) = \int_{\partial D_-} \frac{\partial^2 \Phi(x,y)}{\partial \nu_x \partial \nu_y} u^s_+(y) - \frac{\partial \Phi(x,y)}{\partial \nu_x} \left(\frac{\partial u^s}{\partial \nu_y}\right)_+ (y)\, ds_y + \frac{1}{2}\left(\frac{\partial u^s}{\partial \nu_x}\right)_+ (x), \tag{3.6}$$

$$\left(\frac{\partial u^s}{\partial \nu_x}\right)_- (x) = \int_{\partial D_-} \frac{\partial \Phi(x,y)}{\partial \nu_x} \left(\frac{\partial u^s}{\partial \nu_y}\right)_- (y) - \frac{\partial^2 \Phi(x,y)}{\partial \nu_x \partial \nu_y} u^s_-(y)\, ds_y + \frac{1}{2}\left(\frac{\partial u^s}{\partial \nu_x}\right)_- (x). \tag{3.7}$$

Note that

$$\frac{\partial u(x)}{\partial \nu_x} = \frac{\partial u^i(x)}{\partial \nu_x} + \frac{\partial u^s(x)}{\partial \nu_x}. \tag{3.8}$$

Recall that from (1.5), $\dfrac{\partial u}{\partial \nu_x}$ is continuous across Γ, and $\dfrac{\partial u^i}{\partial \nu_x}$ is continuous in $\mathbb{R}^2$. Therefore, $\dfrac{\partial u^s}{\partial \nu_x}$ is continuous across Γ. $\dfrac{\partial u^s}{\partial \nu_x}$ is continuous across $\tilde{\Gamma}$, which leads to the following continuity condition:

$$\left(\frac{\partial u^s}{\partial \nu_x}\right)_+ = \left(\frac{\partial u^s}{\partial \nu_x}\right)_- \quad \text{on } \partial D_-. \tag{3.9}$$

By adding (3.6) and (3.7), and using (3.9), it is obtained that

$$\frac{\partial u^s(x)}{\partial \nu_x} = \int_\Gamma \frac{\partial^2 \Phi(x,y)}{\partial \nu_x \partial \nu_y} \left[u^s_+(y) - u^s_-(y)\right] \, ds_y, \quad x \in \Gamma.$$

Note that

$$u_+ - u_- = \frac{i\sigma}{k}\sqrt{\frac{\mu_0}{\varepsilon_0}}\frac{\partial u}{\partial \nu} \quad \text{on } \Gamma,$$

and $u_+ - u_- = u^s_+ - u^s_-$ by the continuity of u^i, we arrive at the boundary integral equation,

$$\frac{\partial u(x)}{\partial \nu_x} - \frac{i\sigma}{k}\sqrt{\frac{\mu_0}{\varepsilon_0}} \int_\Gamma \frac{\partial^2 \Phi(x,y)}{\partial \nu_x \partial \nu_y} \frac{\partial u(y)}{\partial \nu_y} \, ds_y = \frac{\partial u^i(x)}{\partial \nu_x}, \quad x \in \Gamma. \tag{3.10}$$

To simplify to the notations, we introduce the following integral operators. For $x \in \Gamma$, we introduce the operators as (2.6)–(2.9).

$$\begin{aligned}
(\tilde{\mathcal{S}}\psi)(x) &:= \int_\Gamma \Phi(x,y)\psi(y) ds_y, \\
(\tilde{\mathcal{K}}\psi)(x) &:= \int_\Gamma \frac{\partial \Phi(x,y)}{\partial \nu_y}\psi(y) ds_y, \\
(\tilde{\mathcal{K}}'\psi)(x) &:= \int_\Gamma \frac{\partial \Phi(x,y)}{\partial \nu_x}\psi(y) ds_y, \\
(\tilde{\mathcal{T}}\psi)(x) &:= \int_\Gamma \frac{\partial^2 \Phi(x,y)}{\partial \nu_x \partial \nu_y}\psi(y) ds_y.
\end{aligned}$$

Let

$$\tau = \sigma\sqrt{\frac{\mu_0}{\varepsilon_0}} \quad \text{and} \quad h = \frac{\partial u^i}{\partial \nu}. \tag{3.11}$$

Then (3.10) can be expressed by

$$\left(\mathcal{I} - \frac{i\tau}{k}\tilde{\mathcal{T}}\right)\frac{\partial u}{\partial \nu} = h. \tag{3.12}$$

The integral operator $\tilde{\mathcal{T}}$ is a hypersingular operator, and is unbounded on $L^2(\Gamma)$ [22, 31, 32, 55]. As such its eigenvalues accumulate at infinity. Therefore, the solution of the discretized integral equation (3.12) by iterative solvers such as the GMRES method would require a large number of iterations.

3.2 Well-posed integral formulation

In this section, we introduce a regularization of the integral equation (3.12) using scaled operators and generalized Calderon formula.

From the classical Calderon formula (2.18) on a closed curve, the composition of the operators $\tilde{\mathcal{S}}$ and $\tilde{\mathcal{T}}$ yields a second integral operator that is well-conditioned. In the context of open surface, the combined operator gives rise to

$$\tilde{\mathcal{T}}\tilde{\mathcal{S}}[1](X) = O\left(\frac{1}{d(X)}\right), \quad X \in \Gamma$$

where $d(X)$ is the distance from the edge of the surface [33]. That is, the image of the constant function under $\tilde{\mathcal{T}}\tilde{\mathcal{S}}$ is singular. Hence $\tilde{\mathcal{T}}\tilde{\mathcal{S}}$ not well-posed anymore.

To address this issue, we apply the idea developed by O. Bruno [8]. Introduce the scaled integral operators

$$\mathcal{S}\psi = \tilde{\mathcal{S}}\left(\psi/\rho\right), \quad \mathcal{T}\psi = \tilde{\mathcal{T}}\left(\rho\psi\right), \tag{3.13}$$

where $\rho \sim O(\sqrt{d})$ near the edge. Without loss of generality, we can choose a smooth parametrization $X(t) = (x(t), y(t))$ of Γ, where $t \in (-1, 1)$, and define the weight function $\rho = \sqrt{1-t^2}$. Then the new integral operators can be expressed as

$$\begin{aligned}
(\mathcal{S}\psi)(X(t)) &= \int_\Gamma \Phi(X(t), X(s))\ \psi(X(s))\ \frac{1}{\sqrt{1-s^2}} dX(s) \\
&= \int_{-1}^{1} \Phi(X(t), X(s))\ \psi(X(s))\ \frac{1}{\sqrt{1-s^2}} |X'(s)|\ ds, \qquad (3.14) \\
(\mathcal{T}\psi)(X(t)) &= \int_\Gamma \frac{\partial^2 \Phi(X(t), X(s))}{\partial \nu_{X(t)} \partial \nu_{X(s)}}\ \psi(X(s))\ \sqrt{1-s^2}\ dX(s) \\
&= \int_{-1}^{1} \frac{\partial^2 \Phi(X(t), X(s))}{\partial \nu_{X(t)} \partial \nu_{X(s)}}\ \psi(X(s))\ \sqrt{1-s^2} |X'(s)|\ ds, \qquad (3.15)
\end{aligned}$$

where $|X'(t)| = \sqrt{\left(\frac{dx(t)}{dt}\right)^2 + \left(\frac{dy(t)}{dt}\right)^2}$.

It can be shown that the following generalized Calderon formula holds (cf. [8]):

$$\mathcal{T}\mathcal{S} = \mathcal{D} + \mathcal{F}. \tag{3.16}$$

In the above, $\mathcal{D}$ is a continuous operator and its eigenvalues are bounded away from zero and infinity, and $\mathcal{F}$ is a compact operator.

Let

$$\frac{\partial u}{\partial \nu}(X(t)) = \sqrt{1-t^2}S\psi.$$

Then the integral equation becomes

$$\mathcal{A}\psi := \left[\sqrt{1-t^2}\mathcal{S} - \frac{i\tau}{k}\mathcal{T}\mathcal{S}\right]\psi = h(X(t)). \tag{3.17}$$

Since $\mathcal{S}$ is a compact operator, $\sqrt{1-t^2}\mathcal{I}$ is a bounded operator, thus $\sqrt{1-t^2}\mathcal{S}$ is a compact operator. According to (3.16), we see that

$$\mathcal{A} = -\frac{i\tau}{k}D + (\sqrt{1-t^2}\mathcal{S} - \frac{i\tau}{k}F).$$

That is, the operator $\mathcal{A}$ is a compact perturbation (given by $\sqrt{1-t^2}\mathcal{S} - \frac{i\tau}{k}F$) from a continuous operator $-\frac{i\tau}{k}D$ whose eigenvalues are bounded away from zero and infinity. Consequently, the eigenvalues of $\mathcal{A}$ are bounded away from zero and infinity.

To illustrate the eigenvalues of the operators $\mathcal{T}$ and $\sqrt{1-t^2}\mathcal{I} - \frac{i\tau}{k}\mathcal{T}$ before and after regularization, we consider the case when Γ is a line segment $[-L, L]$. From Figures 3.2 and 3.3, it is clear that for both $\mathcal{T}$ and $(\sqrt{1-t^2}\mathcal{I} - \frac{i\tau}{k}\mathcal{T})$, the eigenvalues with smaller modulus accumulate at zero and the eigenvalues with larger modulus tend to infinity. However, the eigenvalues for the regularized integral operators $\mathcal{T}\mathcal{S}$ and $\mathcal{A}$ accumulate at a nonzero value.

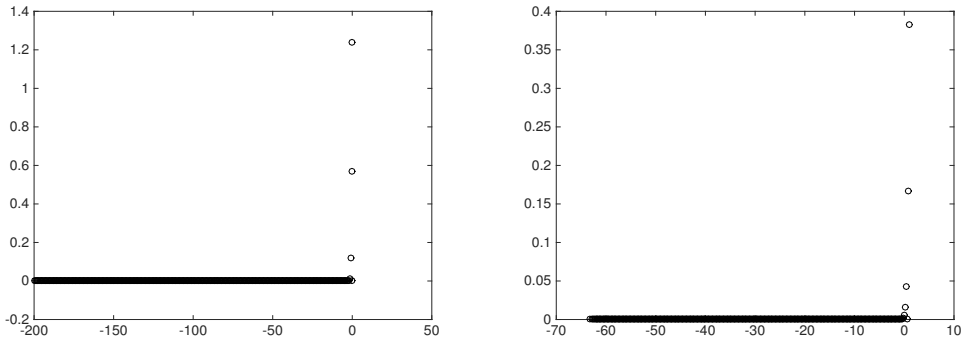

Figure 3.2: Eigenvalues of $\mathcal{T}$ and $\sqrt{1-t^2}\mathcal{I} - \dfrac{i\tau}{k}\mathcal{T}$ when $k = \pi$, $L = 50$, and $\tau = 0.02i$.

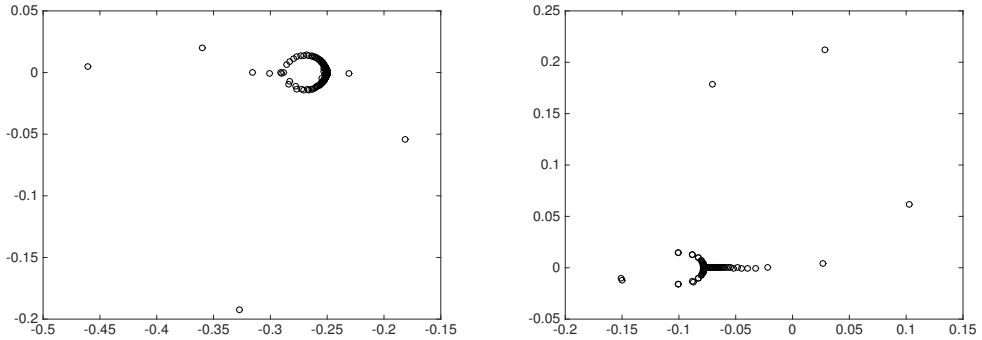

Figure 3.3: Eigenvalues of $\mathcal{TS}$ and A when $k = \pi$, $L = 50$, and $\tau = 0.02i$.

Chapter 4

Nystrom discretization scheme

In this chapter, we apply the Nystrom decretization method to discretize the integral equation (3.17). More precisely, we use the Chebyshev polynomial interpolant to approximate the unknown function, and evaluate the integral with the logarithmic kernel analytically. To this end, we first introduce Chebyshev polynomials and Chebyshev interpolations, and then discuss the evaluation of the integral operators using Chebyshev polynomial interpolation.

4.1 Chebyshev polynomials

In this section, we introduce Chebyshev polynomials and collect several important properties for Chebyshev polynomials. We refer to [43] for more details.

For $x \in [-1, 1]$, the Chebyshev polynomial of degree n, denoted by $T_n(x)$, is defined as

$$T_n(x) = \cos(n \arccos x). \tag{4.1}$$

Let $\theta = \arccos x$, then $\theta \in [0, \pi]$ and $T_n(x) = \cos(n\theta)$.

The first few Chebyshev polynomials are explicitly given as

$$T_0(x) = 1, \quad T_1(x) = x, \quad T_2(x) = 2x^2 - 1,$$
$$T_3(x) = 4x^3 - 3x, \quad T_4(x) = 8x^4 - 8x^2 + 1, \cdots$$

From the trigonometric identities, $T_n(x)$ satisfies the following recurrence relation:

$$T_n(x) = 2xT_{n-1}(x) - T_{n-2}(x), \quad n = 2, 3, \cdots$$

The zeros of $T_n(x)$ for x in $[-1, 1]$ correspond to the zeros for θ in $[0, \pi]$ of $\cos n\theta$, which are

$$n\theta = \left(k - \frac{1}{2}\right)\pi, \quad k = 1, 2, \cdots, n.$$

Hence the zeros of $T_n(x)$ are

$$x_k = \cos\frac{(2k-1)\pi}{2n}, \quad k = 1, 2, \cdots, n.$$

The extrema of $T_n(x)$ occur at $n\theta = k\pi$, that is,

$$x = \cos\frac{k\pi}{n}, \quad k = 0, 1, \cdots, n$$

In the following, we state the orthogonality of Chebyshev polynomials.

Definition 4.1 *Two functions $f(x)$ and $g(x)$ in $\mathcal{L}_2[a, b]$ are orthogonal on the interval $[a, b]$ with respect to a given continuous and non-negative weight function $w(x)$ if*

$$\int_a^b w(x)f(x)g(x)\,dx = 0.$$

The above formula can be written in the "inner product" notation as

$$\langle f, g\rangle = \int_a^b w(x)f(x)g(x)\,dx = 0.$$

The Chebyshev polynomials $\{T_n,\ n = 0, 1, \cdots\}$ form an orthogonal polynomial system on $[-1, 1]$ with respect to the weight $w(x) = (1 - x^2)^{-\frac{1}{2}}$ [43]. That is,

$$\langle T_n, T_m\rangle = \int_{-1}^{1} \frac{T_n(x)T_m(x)}{\sqrt{1-x^2}}\,dx = 0, \quad n \neq m. \tag{4.2}$$

Moreover, $||T_0||^2 = \langle T_0, T_0 \rangle = \pi$, and

$$||T_n||^2 = \langle T_n, T_n \rangle = \frac{1}{2}\pi \quad \text{for } n \neq 0.$$

Given a function $f(x)$, we expand it using the Chebyshev polynomials $\{T_n(x)\}_{n=0}^{\infty}$, which takes the form of

$$f(x) = \sum_{n=0}^{\infty} c_n T_n(x), \quad x \in [-1, 1]. \tag{4.3}$$

By taking the inner product with $T_m(x)$ and using the orthogonality, we see that

$$\langle f, T_m \rangle = \sum_{n=0}^{\infty} c_n \langle T_n, T_m \rangle = c_m \langle T_m, T_m \rangle, \tag{4.4}$$

thus the coefficient c_m can be expressed as

$$c_n = \frac{\langle f, T_n \rangle}{\langle T_n, T_n \rangle}. \tag{4.5}$$

The following theorem states that the expansion (4.3) holds when f is a continuous function on $[-1, 1]$ (cf. [43]).

Theorem 4.1 *If f is continuous on $[a, b]$, then the expansion* (4.3) *in Chebyshev polynomials converges in $\mathcal{L}_2$ with respect to the weight function $w(x) = (1 - x^2)^{-\frac{1}{2}}$.*

4.2 Chebyshev polynomial interpolation

For a function $f(x) \in H^s(-1, 1)$, we sample the function values at zeros of Chebyshev polynomial $T_N(x)$,

$$x_n = \cos \frac{(2n-1)\pi}{2N} \text{ or } \theta_n = \frac{(2n-1)\pi}{2N}, \quad n = 1, 2, \cdots, N.$$

The corresponding Chebyshev polynomial $P_N(x)$ with degree $N - 1$ to approximate $f(x)$ is given by (cf. [48])

$$P_N(x) = \sum_{n=1}^{N-1} c_n T_n(x) + \frac{c_0}{2}, \tag{4.6}$$

where

$$c_n = \frac{2}{N}\sum_{j=1}^{N} f(x_j)T_n(x_j), \quad n = 0, 1, \cdots, N-1. \tag{4.7}$$

The above approximation can be written in the θ coordinate as follows:

$$P_N(\theta) = \sum_{n=1}^{N-1} c_n \cos(n\theta) + \frac{c_0}{2}, \tag{4.8}$$

where

$$\begin{aligned} c_n &= \frac{2}{N}\sum_{j=1}^{N} g(\theta_j)\cos(n\theta_j), \quad n = 0, 1, \cdots, N-1. \\ g(\theta_j) &= f(x_j). \end{aligned} \tag{4.9}$$

Therefore, the relationship between c_n and $g(\theta_j)$ can be written in the matrix form as follows:

$$\begin{aligned} \begin{pmatrix} c_0 \\ c_1 \\ \vdots \\ c_{N-1} \end{pmatrix} &= \frac{2}{N} \begin{pmatrix} 1 & \cdots & 1 \\ \cos\theta_1 & \cdots & \cos\theta_N \\ & \ddots & \\ \cos(N-1)\theta_1 & \cdots & \cos(N-1)\theta_N \end{pmatrix} \begin{pmatrix} g(\theta_1) \\ g(\theta_2) \\ \vdots \\ g(\theta_N) \end{pmatrix} \\ &= \frac{2}{N} \cdot B \cdot \begin{pmatrix} g(\theta_1) \\ g(\theta_2) \\ \vdots \\ g(\theta_N) \end{pmatrix}, \end{aligned} \tag{4.10}$$

where

$$B = \begin{pmatrix} 1 & \cdots & 1 \\ \cos\theta_1 & \cdots & \cos\theta_N \\ & \ddots & \\ \cos(N-1)\theta_1 & \cdots & \cos(N-1)\theta_N \end{pmatrix}. \tag{4.11}$$

By substituting (4.9) into (4.8), it follows that

$$P_N(\theta) = \sum_{j=1}^{N} g(\theta_j) L_j(\theta), \tag{4.12}$$

where

$$L_j(\theta) = \frac{1}{N} + \frac{2}{N} \sum_{n=1}^{N-1} \cos(n\theta_j) \cos(n\theta). \tag{4.13}$$

Note that $L_j(\theta)$ is the Lagrange basis function associated with the interpolation points $\theta_n = \dfrac{(2n-1)\pi}{2N}$ $(n = 1, 2, \cdots, N)$.

Let $P_N(x)$ be the Chebyshev polynomial interpolant for $f(x)$ given by (4.6), then the following polynomial of degree $N-2$ serves as an approximation for $\dfrac{df(x)}{dx}$:

$$P'_{N-2}(x) = \sum_{n=1}^{N-2} c'_n T_n(x) + \frac{c'_0}{2}, \tag{4.14}$$

where the relationship between c_n and c'_n are given as follows [48]:

$$\begin{cases} c'_{n-1} = c'_{n+1} + 2nc_n, \quad n = 1, 2, \cdots, N-1 \\ c'_N = c'_{N-1} = 0. \end{cases} \tag{4.15}$$

From the above recurrence relation, we can express c'_n in terms of c_n explicitly. If N is odd, it follows that

$$\begin{cases} c'_{N-2} = c'_N + 2(N-1)c_{N-1} = 2(N-1)c_{N-1}, \\ c'_{N-3} = c'_{N-1} + 2(N-2)c_{N-2} = 2(N-2)c_{N-2}, \\ c'_{N-4} = c'_{N-2} + 2(N-3)c_{N-3} = 2(N-1)c_{N-1} + 2(N-3)c_{N-3}, \\ \cdots \\ c'_1 = c'_3 + 4c_2 = 2(N-1)c_{N-1} + 2(N-3)c_{N-3} + \cdots + 8c_4 + 4c_2, \\ c'_0 = c'_2 + 2c_1 = 2(N-2)c_{N-2} + 2(N-4)c_{N-4} + \cdots + 6c_3 + 2c_1. \end{cases}$$

When N is even, then

$$\begin{cases} c'_{N-2} = c'_N + 2(N-1)c_{N-1} = 2(N-1)c_{N-1}, \\ c'_{N-3} = c'_{N-1} + 2(N-2)c_{N-2} = 2(N-2)c_{N-2}, \\ c'_{N-4} = c'_{N-2} + 2(N-3)c_{N-3} = 2(N-1)c_{N-1} + 2(N-3)c_{N-3}, \\ \cdots \\ c'_1 = c'_3 + 4c_2 = 2(N-2)c_{N-2} + 2(N-4)c_{N-4} + \cdots + 8c_4 + 4c_2, \\ c'_0 = c'_2 + 2c_1 = 2(N-1)c_{N-1} + 2(N-3)c_{N-3} + \cdots + 6c_3 + 2c_1. \end{cases}$$

Now let

$$\mathbf{c}' = [c'_0, c'_1, \cdots, c'_{N-2}]' \quad \text{and} \quad \mathbf{c} = [c_0, c_1, \cdots, c_{N-2}, c_{N-1}]'.$$

We may write the above equations in the matrix form as follows. If N is odd,

$$\mathbf{c}' = 2 \begin{pmatrix} 0 & 1 & 0 & 3 & 0 & \cdots & N-2 & 0 \\ 0 & 0 & 2 & 0 & 4 & \cdots & 0 & N-1 \\ & & & & & \ddots & & \\ 0 & 0 & 0 & 0 & \cdots & N-3 & 0 & N-1 \\ 0 & 0 & 0 & 0 & 0 & \cdots & N-2 & 0 \\ 0 & 0 & 0 & 0 & 0 & \cdots & 0 & N-1 \end{pmatrix} \cdot \mathbf{c} \tag{4.16}$$

If N is even,

$$\mathbf{c}' = 2 \begin{pmatrix} 0 & 1 & 0 & 3 & 0 & \cdots & 0 & N-1 \\ 0 & 0 & 2 & 0 & 4 & \cdots & N-2 & 0 \\ & & & & & \ddots & & \\ 0 & 0 & 0 & 0 & \cdots & N-3 & 0 & N-1 \\ 0 & 0 & 0 & 0 & 0 & \cdots & N-2 & 0 \\ 0 & 0 & 0 & 0 & 0 & \cdots & 0 & N-1 \end{pmatrix} \cdot \mathbf{c} \tag{4.17}$$

We define the matrix P by

$$P = \begin{pmatrix} 0 & 1 & 0 & 3 & 0 & \cdots & N-2 & 0 \\ 0 & 0 & 2 & 0 & 4 & \cdots & 0 & N-1 \\ & & & & & \ddots & & \\ 0 & 0 & 0 & 0 & \cdots & N-3 & 0 & N-1 \\ 0 & 0 & 0 & 0 & 0 & \cdots & N-2 & 0 \\ 0 & 0 & 0 & 0 & 0 & \cdots & 0 & N-1, \end{pmatrix}$$

and

$$P = \begin{pmatrix} 0 & 1 & 0 & 3 & 0 & \cdots & 0 & N-1 \\ 0 & 0 & 2 & 0 & 4 & \cdots & N-2 & 0 \\ & & & & & \ddots & & \\ 0 & 0 & 0 & 0 & \cdots & N-3 & 0 & N-1 \\ 0 & 0 & 0 & 0 & 0 & \cdots & N-2 & 0 \\ 0 & 0 & 0 & 0 & 0 & \cdots & 0 & N-1 \end{pmatrix}.$$

for odd and even n respectively.

4.3 Evaluation of integral operators

In this section, we derive the evaluation of the integral operator $\mathcal{S}$ and $\mathcal{T}$ given in Chapter 3. To give a more clear picture, we first consider the case when Γ is a line segment, then we derive the formulas when Γ is an open curve.

4.3.1 Flat graphene sheets

In this subsection, the graphene is assumed to be a flat sheet such that Γ is the line segment $[-L, L]$.

From (3.14) and (3.15), let $t = \cos\theta, then X(t) = (L\cos\theta, 0)$ and $\phi(\theta) = \psi(X(t))$, where $\theta \in [0, \pi]$. Correspondingly, the operators $\mathcal{S}$ and $\mathcal{T}$ in terms of θ are

$$(\mathcal{S}\phi)(\theta) = L\int_0^\pi \Phi(\cos\theta, 0; \cos\theta', 0)\ \phi(\theta')\ d\theta', \tag{4.18}$$

$$(\mathcal{T}\phi)(\theta) = L\int_0^\pi \frac{\partial^2\Phi(\cos\theta, 0; \cos\theta', 0)}{\partial\nu_{X(\theta)}\partial\nu_{X(\theta')}}\ \phi(\theta')\ \sin^2(\theta')\ d\theta'. \tag{4.19}$$

In the following, we evaluate $\mathcal{S}\phi$ explictly. First, we expand the kernel Φ as follows (cf. [8]):

$$\begin{aligned}\Phi(\cos\theta, 0; \cos\theta', 0) &= \frac{i}{4}H_0^{(1)}(k|\cos\theta - \cos\theta'|) \\ &= M_1(\theta, \theta')\ln|\cos\theta - \cos\theta'| + M_2(\theta, \theta').\end{aligned} \tag{4.20}$$

where

$$M_1(\theta, \theta') = -\frac{1}{2\pi}J_0^{(1)}(k|\cos\theta - \cos\theta'|),$$

and

$$M_2(\theta, \theta') = \frac{i}{4}H_0^{(1)}(k|\cos\theta - \cos\theta'|) + \frac{1}{2\pi}J_0^{(1)}(k|\cos\theta - \cos\theta'|).$$

Note that $M_1(\theta, \theta')$ and $M_2(\theta, \theta')$ are smooth functions, therefore, the singularity of $\Phi(\cos\theta, 0; \cos\theta', 0)$ resides in the term $\ln|\cos\theta - \cos\theta'|$.

From (4.18) and (4.20), we obtain

$$\begin{aligned}(\mathcal{S}\phi)(\theta) &= L\int_0^\pi \Phi(\cos\theta, 0; \cos\theta', 0)\ \phi(\theta')\ d\theta', \\ &= L\int_0^\pi \ln|\cos\theta - \cos\theta'|M_1(\theta, \theta')\phi(\theta') + M_2(\theta, \theta')\phi(\theta')\ d\theta,\end{aligned} \tag{4.21}$$

where $\displaystyle\int_0^\pi \ln|\cos\theta - \cos\theta'|M_1(\theta, \theta')\phi(\theta')\ d\theta$ is a weakly singular integral and $\displaystyle\int_0^\pi M_2(\theta, \theta')\phi(\theta')\ d\theta$ is a smooth integral.

In order to evaluate $\int_0^\pi \ln|\cos\theta-\cos\theta'|M_1(\theta,\theta')\phi(\theta')\,d\theta$, we use the following formulas for cosine functions (cf. [9]):

$$\begin{cases} \displaystyle\int_0^\pi \ln|\cos\theta-\cos\theta'|\,d\theta' = -\pi\ln 2 =: \ell_0, \\ \displaystyle\int_0^\pi \ln|\cos\theta-\cos\theta'|\,\cos(n\theta')\,d\theta' = -\frac{\pi}{n}\cos n\theta =: \ell_n\cos n\theta. \end{cases} \tag{4.22}$$

We use the Chebyshev polynomial interpolant $P_N(\theta')$ to approximate $M_1(\theta,\theta')\phi(\theta')$ as a function of θ'. Therefore, by (4.12), (4.13) and (4.22), it follows that

$$\begin{aligned} & \int_0^\pi \ln|\cos\theta-\cos\theta'|M_1(\theta,\theta')\phi(\theta')\,d\theta \\ \approx\ & \int_0^\pi \left[\sum_{j=1}^N M_1(\theta,\theta_j)\phi(\theta_j)L_j(\theta')\right]\cdot\ln|\cos\theta-\cos\theta'|\,d\theta \\ =\ & \sum_{j=1}^N M_1(\theta,\theta_j)\phi(\theta_j)\int_0^\pi L_j(\theta')\ln|\cos\theta-\cos\theta'|\,d\theta \\ =\ & \sum_{j=1}^N M_1(\theta,\theta_j)\phi(\theta_j)\left[\frac{\ell_0}{N}+\frac{2}{N}\sum_{n=1}^{N-1}\ell_n\cos(n\theta_j)\cos(n\theta)\right] \\ =:\ & \sum_{j=1}^N M_1(\theta,\theta_j)\phi(\theta_j)R_j(\theta). \end{aligned} \tag{4.23}$$

Note that by using (4.22), no numerical quadrature is needed for evaluating this singular integral.

To evaluate $\int_0^\pi M_2(\theta,\theta')\phi(\theta')\,d\theta$, we use the fact that

$$\int_0^\pi L_j(\theta')\,d\theta' = \frac{\pi}{N}. \tag{4.24}$$

Similarly, we approximate $M_2(\theta,\theta')\phi(\theta')$ as a function of θ' by the Chebyshev polynomials. From (4.12) and (4.24), it follows that

$$\begin{aligned} \int_0^\pi M_2(\theta,\theta')\phi(\theta')\,d\theta \ &\approx\ \int_0^\pi \sum_{j=1}^N M_2(\theta,\theta_j)\phi(\theta_j)L_j(\theta')\,d\theta \\ &=\ \frac{\pi}{N}\sum_{j=1}^N M_2(\theta,\theta_j)\phi(\theta_j). \end{aligned} \tag{4.25}$$

Hence, combining (4.21), (4.23) and (4.25), we arrive at

$$\begin{aligned}(\mathcal{S}\phi)(\theta) &= L\int_0^{\pi}\Phi(\cos\theta,0;\cos\theta',0)\ \phi(\theta)\ d\theta' \\ &\approx L\left[\sum_{j=1}^{N}R_j(\theta)M_1(\theta,\theta_j)\phi(\theta_j)+\frac{\pi}{N}\sum_{j=1}^{N}M_2(\theta,\theta_j)\phi(\theta_j)\right].\end{aligned} \tag{4.26}$$

Let

$$\mathbf{S_L}(\theta)=\left[\ R_1(\theta)M_1(\theta,\theta_1)+\frac{\pi}{N}M_2(\theta,\theta_1),\quad\cdots,\quad R_N(\theta)M_1(\theta,\theta_N)+\frac{\pi}{N}M_2(\theta,\theta_N)\ \right],$$

then the estimate of $\mathcal{S}\phi$ can be written in the matrix form as:

$$(\mathcal{S}\phi)(\theta)\approx L\mathbf{S_L}(\theta)\begin{pmatrix}\phi(\theta_1)\\ \phi(\theta_2)\\ \vdots\\ \phi(\theta_N)\end{pmatrix}. \tag{4.27}$$

This completes the evaluation of $\mathcal{S}\phi$.

We discuss the evaluation of $\mathcal{T}$ in the remainder of the subsection. From (3.15), we can see that the kernel is the second derivative of fundamental solution, therefore it is hard to evaluate directly. However, $\mathcal{T}$ can be decomposed into (cf. [14])

$$\mathcal{T}=\mathcal{T}^g+\mathcal{T}^s, \tag{4.28}$$

where

$$(\mathcal{T}^g\psi)(X(t))=k^2\int_{-1}^{1}\Phi(X(t),X(s))\ \psi(X(s))\ |X'(s)|\ \sqrt{1-s^2}\ (\nu_{X(t)}\cdot\nu_{X(s)})\ ds,$$

and

$$(\mathcal{T}^s\psi)(X(t))=\frac{1}{|X'(t)|}\frac{d}{dt}\int_{-1}^{1}\Phi(X(t),X(s))\ \frac{d}{ds}(\psi(X(s))\ \sqrt{1-s^2})\ ds.$$

In the case of a line segment, $\mathcal{T}^g$ in the θ coordinate can be reduced to

$$(\mathcal{T}^g\phi)(\theta) \;=\; k^2 L \int_0^\pi \Phi(\cos\theta, 0; \cos\theta', 0)\ \phi(\theta')\ \sin^2(\theta')\ d\theta'.$$

From (4.18), it is obvious that

$$(\mathcal{T}^g\phi)(\theta) = k^2 \cdot \mathcal{S}(\psi)(\theta),$$

where

$$\psi(\theta) = \phi(\theta)\sin^2(\theta).$$

From above discussion, we already know how to evaluate $\mathcal{S}$, thus we are able to evaluate $\mathcal{T}^g$ as follows:

$$(\mathcal{T}^g\phi)(\theta) \;\approx\; k^2 L \left[\sum_{j=1}^{N} R_j(\theta) M_1(\theta,\theta_j)\sin^2(\theta_j)\phi(\theta_j) + \frac{\pi}{N}\sum_{j=1}^{N} M_2(\theta,\theta_j)\sin^2(\theta_j)\phi(\theta_j)\right].$$

Let

$$\mathbf{S_{TgL}}(\theta) = \begin{pmatrix} R_1(\theta)M_1(\theta,\theta_1)\sin^2(\theta_1) + \dfrac{\pi}{N}M_2(\theta,\theta_1)\sin^2(\theta_1) \\ R_2(\theta)M_1(\theta,\theta_2)\sin^2(\theta_2) + \dfrac{\pi}{N}M_2(\theta,\theta_2)\sin^2(\theta_2) \\ \vdots \\ R_N(\theta)M_1(\theta,\theta_N)\sin^2(\theta_N) + \dfrac{\pi}{N}M_2(\theta,\theta_N)\sin^2(\theta_N) \end{pmatrix}^{\mathrm{T}},$$

then

$$(\mathcal{T}^g\phi)(\theta) \approx k^2 L\ \mathbf{S_{TgL}}(\theta) \begin{pmatrix} \phi(\theta_1) \\ \phi(\theta_2) \\ \vdots \\ \phi(\theta_N) \end{pmatrix}. \tag{4.29}$$

The remaining task is to evaluate $\mathcal{T}^s$. We write $\mathcal{T}^s$ in the θ coordinate and have

$$(\mathcal{T}^s\phi)(\theta) \;=\; \frac{1}{L\sin\theta}\frac{d}{d\theta}\int_0^\pi \Phi(\cos\theta, 0; \cos\theta', 0)\ \frac{d}{d\theta'}(\phi(\theta')\ \sin\theta')\ d\theta'.$$

It can be viewed as the composition of three operators given by

$$(\mathcal{T}^s\phi)(\theta) = \frac{1}{L}(\mathcal{T}_1 \cdot \mathcal{S} \cdot \mathcal{T}_2)\ (\phi(\theta) \cdot \sin\theta). \tag{4.30}$$

Here

$$\mathcal{T}_1 := \frac{1}{\sin\theta}\frac{d}{d\theta}, \quad \mathcal{T}_2 := \frac{d}{d\theta}.$$

Recalling the change of variables for $t = \cos\theta$, it follows that

$$\mathcal{T}_1 = \frac{1}{\sin\theta}\frac{d}{d\theta} = -\frac{d}{dt}.$$

To evaluate $\mathcal{T}_1 f(X(t))$, we use the Chebyshev polynomial interpolant to approximate $f(X(t))$. From the formula of Chebyshev polynomial interpolant (4.14) and its derivative (4.15), we have

$$\mathcal{T}_1 f(X(t)) = -\frac{d}{dt}f(X(t)) \approx -\left(\sum_{n=1}^{N-2} c'_n T_n(t) + \frac{c'_0}{2}\right).$$

To express $\mathcal{T}_1 f(X(t))$ in terms of interpoation values, we let $f(X(t)) = g(\theta)$. It is clear that the interpolant values are $\{\theta_j, g(\theta_j)\}_{j=1}^N$. Recall that the relationship between c'_n and c_n are given by (4.15), (4.16) and (4.17). Thus from (4.10), we obtain

$$\begin{aligned} & \sum_{n=1}^{N-2} c'_n T_n(t) + \frac{c'_0}{2} \\ = & \sum_{n=1}^{N-2} c'_n \cos(n\theta) + \frac{c'_0}{2} \\ = & \begin{pmatrix} \frac{1}{2} & \cos\theta & \cdots & \cos(N-2)\theta \end{pmatrix} \cdot \begin{pmatrix} c'_0 \\ c'_1 \\ \vdots \\ c'_{N-2} \end{pmatrix} \end{aligned} \tag{4.31}$$

$$
\begin{aligned}
&= \left(\begin{array}{cccc} \frac{1}{2} & \cos\theta & \cdots & \cos(N-2)\theta \end{array} \right) \cdot P \cdot \left(\begin{array}{c} c_0 \\ c_1 \\ \vdots \\ c_{N-1} \end{array} \right) \\
&= \frac{2}{N} \left(\begin{array}{cccc} \frac{1}{2} & \cos\theta & \cdots & \cos(N-2)\theta \end{array} \right) \cdot PB \cdot \left(\begin{array}{c} g(\theta_1) \\ g(\theta_2) \\ \vdots \\ g(\theta_N) \end{array} \right).
\end{aligned}
$$

Here the matrix P is given by (4.16) and (4.17), and the matrix B is given by (4.11). Define

$$
\mathbf{T_{1Lb}}(\theta) = \left(\begin{array}{cccc} \frac{1}{2} & \cos\theta & \cdots & \cos(N-2)\theta \end{array} \right).
$$

Then the evaluation of $\mathcal{T}_1$ can be expressed as the following matrix form:

$$
\mathcal{T}_1 g(\theta) \approx -\frac{2}{N} \mathbf{T_{1Lb}}(\theta) \cdot P \cdot B \cdot \left(\begin{array}{c} g(\theta_1) \\ g(\theta_2) \\ \vdots \\ g(\theta_N) \end{array} \right). \tag{4.32}
$$

Next, we discuss the evaluation of $\mathcal{T}_2(g(\theta)\sin\theta) = \dfrac{d}{d\theta}(g(\theta)\sin\theta)$. Approximating $g(\theta)$ by the Chebyshev polynomial (4.8) and using the product-to-sum identity, we have

$$
\begin{aligned}
\frac{d}{d\theta}(g(\theta)\sin\theta) &\approx \frac{d}{d\theta}\left(\left(\sum_{n=1}^{N-1} c_n \cos(n\theta) + \frac{c_0}{2} \right) \sin\theta \right) \\
&= \frac{d}{d\theta}\left(\sum_{n=1}^{N-1} \frac{c_n}{2} [\sin(n+1)\theta - \sin(n-1)\theta] + \frac{c_0}{2}\sin\theta \right) \\
&= \sum_{n=1}^{N-1} \frac{c_n}{2} [(n+1)\cos(n+1)\theta - (n-1)\cos(n-1)\theta] + \frac{c_0}{2}\cos\theta
\end{aligned}
$$

$$
\begin{aligned}
&= \frac{1}{2}\left(\begin{array}{ccc} \cos\theta & \cdots & N\cos N\theta - (N-2)\cos(N-2)\theta \end{array} \right) \cdot \left(\begin{array}{c} c_0 \\ c_1 \\ \vdots \\ c_{N-1} \end{array} \right) \\
&= \frac{1}{2}\left(\begin{array}{ccc} \cos\theta & \cdots & N\cos N\theta - (N-2)\cos(N-2)\theta \end{array} \right) B \left(\begin{array}{c} g(\theta_1) \\ g(\theta_2) \\ \vdots \\ g(\theta_N) \end{array} \right).
\end{aligned}
$$

Let

$$
\mathbf{T_{2Lb}}(\theta) = \left(\begin{array}{ccc} \cos\theta & \cdots & N\cos N\theta - (N-2)\cos(N-2)\theta \end{array} \right),
$$

we obtain

$$
\mathcal{T}_2(\phi(\theta)\sin\theta) \approx \frac{1}{2}\mathbf{T_{2Lb}}(\theta) \cdot B \cdot \left(\begin{array}{c} \phi(\theta_1) \\ \phi(\theta_2) \\ \vdots \\ \phi(\theta_N) \end{array} \right). \tag{4.33}
$$

Now we are ready to evaluate $(\mathcal{T}^s\phi)(\theta)$. From (4.30) and (4.32),

$$
\begin{aligned}
(\mathcal{T}^s\phi)(\theta) &= \frac{1}{L}(\mathcal{T}_1 \cdot \mathcal{S} \cdot \mathcal{T}_2)\ (\phi(\theta) \cdot \sin\theta) \\
&\approx -\frac{2}{NL}\mathbf{T_{1Lb}}(\theta) PB \left(\begin{array}{c} \mathcal{S}\mathcal{T}_2(\phi(\theta_1)\sin\theta_1) \\ \mathcal{S}\mathcal{T}_2(\phi(\theta_2)\sin\theta_2) \\ \vdots \\ \mathcal{S}\mathcal{T}_2(\phi(\theta_N)\sin\theta_N \end{array} \right).
\end{aligned}
$$

For $\mathcal{ST}_2(\phi(\theta_i)\sin\theta_i)$, by (4.27), we see that

$$\mathcal{ST}_2(\phi(\theta_i)\sin\theta_i) \approx L\mathbf{S_L}(\theta_i)\begin{pmatrix} \mathcal{T}_2(\phi(\theta_1)\sin\theta_1) \\ \mathcal{T}_2(\phi(\theta_2)\sin\theta_2) \\ \vdots \\ \mathcal{T}_2(\phi(\theta_N)\sin\theta_N) \end{pmatrix}.$$

By (4.33), it is obvious that

$$\mathcal{T}_2(\phi(\theta_i)\sin\theta_i) \approx \frac{1}{2}\mathbf{T_{2Lb}}(\theta_i)\cdot B\cdot\begin{pmatrix} \phi(\theta_1) \\ \phi(\theta_2) \\ \vdots \\ \phi(\theta_N) \end{pmatrix}.$$

Therefore, the evaluation of $\mathcal{T}^s(\phi)$ can be summarized as follows:

$$\begin{aligned}
(\mathcal{T}^s\phi)(\theta) &\approx -\frac{2}{NL}\mathbf{T_{1Lb}}(\theta)PB\begin{pmatrix} \mathcal{ST}_2(\phi(\theta_1)\sin\theta_1) \\ \mathcal{ST}_2(\phi(\theta_2)\sin\theta_2) \\ \vdots \\ \mathcal{ST}_2(\phi(\theta_N)\sin\theta_N \end{pmatrix} \\
&\approx -\frac{2}{N}\mathbf{T_{1Lb}}(\theta)PB\begin{pmatrix} \mathbf{S_L}(\theta_1) \\ \mathbf{S_L}(\theta_2) \\ \vdots \\ \mathbf{S_L}(\theta_N) \end{pmatrix}\begin{pmatrix} \mathcal{T}_2(\phi(\theta_1)\sin\theta_1) \\ \mathcal{T}_2(\phi(\theta_2)\sin\theta_2) \\ \vdots \\ \mathcal{T}_2(\phi(\theta_N)\sin\theta_N) \end{pmatrix} \\
&\approx -\frac{1}{N}\mathbf{T_{1Lb}}(\theta)PB\begin{pmatrix} \mathbf{S_L}(\theta_1) \\ \mathbf{S_L}(\theta_2) \\ \vdots \\ \mathbf{S_L}(\theta_N) \end{pmatrix}\begin{pmatrix} \mathbf{T_{2Lb}}(\theta_1) \\ \mathbf{T_{2Lb}}(\theta_2) \\ \vdots \\ \mathbf{T_{2Lb}}(\theta_N) \end{pmatrix}B\begin{pmatrix} \phi(\theta_1) \\ \phi(\theta_2) \\ \vdots \\ \phi(\theta_N) \end{pmatrix}. \quad (4.34)
\end{aligned}$$

Let us define

$$\mathbf{T_{sL}} = PB \begin{pmatrix} \mathbf{S_L}(\theta_1) \\ \mathbf{S_L}(\theta_2) \\ \vdots \\ \mathbf{S_L}(\theta_N) \end{pmatrix} \begin{pmatrix} \mathbf{T_{2Lb}}(\theta_1) \\ \mathbf{T_{2Lb}}(\theta_2) \\ \vdots \\ \mathbf{T_{2Lb}}(\theta_N) \end{pmatrix} B.$$

Then

$$(\mathcal{T}^s\phi)(\theta) \approx -\frac{1}{N}\mathbf{T_{1Lb}}(\theta)\mathbf{T_{sL}} \begin{pmatrix} \phi(\theta_1) \\ \phi(\theta_2) \\ \vdots \\ \phi(\theta_N) \end{pmatrix}. \tag{4.35}$$

To evaluate the operators in the boundary integral equation (3.17), note that in θ coordinate it takes the form of

$$\mathcal{A}\phi(\theta) = \left[\sin\theta\ \mathcal{S} - \frac{i\tau}{k}\mathcal{T}\mathcal{S}\right]\phi(\theta) = \tilde{h}(\theta).$$

Combining (4.27), (4.29) and (4.35), we see that

$$\begin{aligned} (\mathcal{T}\mathcal{S}\phi)(\theta) &= (\mathcal{T}^g + \mathcal{T}^s)(\mathcal{S}\phi)(\theta) \\ &\approx \left[k^2 L\mathbf{S_{TgL}}(\theta) - \frac{1}{N}\mathbf{T_{1Lb}}(\theta)\mathbf{T_{sL}}\right] \begin{pmatrix} (\mathcal{S}\phi)(\theta_1) \\ (\mathcal{S}\phi)(\theta_2) \\ \vdots \\ (\mathcal{S}\phi)(\theta_N) \end{pmatrix} \\ &\approx \left[k^2 L\mathbf{S_{TgL}}(\theta) - \frac{1}{N}\mathbf{T_{1Lb}}(\theta)\mathbf{T_{sL}}\right] L \begin{pmatrix} \mathbf{S_L}(\theta_1) \\ \mathbf{S_L}(\theta_2) \\ \vdots \\ \mathbf{S_L}(\theta_N) \end{pmatrix} \begin{pmatrix} \phi(\theta_1) \\ \phi(\theta_2) \\ \vdots \\ \phi(\theta_N) \end{pmatrix}. \end{aligned} \tag{4.36}$$

Define

$$\mathbf{TS}_c(\theta) = \left[k^2 L \mathbf{S}_{\mathbf{TgL}}(\theta) - \frac{1}{N}\mathbf{T}_{\mathbf{1Lb}}(\theta)\mathbf{T}_{\mathbf{sL}}\right] L \begin{pmatrix} \mathbf{S}_{\mathbf{L}}(\theta_1) \\ \mathbf{S}_{\mathbf{L}}(\theta_2) \\ \vdots \\ \mathbf{S}_{\mathbf{L}}(\theta_N) \end{pmatrix}.$$

Then the discretization of $\mathcal{A}\phi$ in (3.17) leads to the following equation

$$\left[L \sin\theta \mathbf{S}_{\mathbf{L}}(\theta) - \frac{i\tau}{k}\mathbf{TS}_c(\theta)\right] \begin{pmatrix} \phi(\theta_1) \\ \phi(\theta_2) \\ \vdots \\ \phi(\theta_N) \end{pmatrix} = \tilde{h}(\theta).$$

In order to solve for $\phi(\theta_1), \phi(\theta_2), \cdots, \phi(\theta_N)$, we choose collocation points at Chebyshev points $\theta_1, \theta_2, \cdots, \theta_N$. We finally arrive at the following linear system when Γ is a line segment:

$$\begin{pmatrix} L\sin\theta_1 \mathbf{S}_{\mathbf{L}}(\theta_1) - \frac{i\tau}{k}\mathbf{TS}_c(\theta_1) \\ L\sin\theta_2 \mathbf{S}_{\mathbf{L}}(\theta_2) - \frac{i\tau}{k}\mathbf{TS}_c(\theta_2) \\ \vdots \\ L\sin\theta_N \mathbf{S}_{\mathbf{L}}(\theta_N) - \frac{i\tau}{k}\mathbf{TS}_c(\theta_N) \end{pmatrix} \begin{pmatrix} \phi(\theta_1) \\ \phi(\theta_2) \\ \vdots \\ \phi(\theta_N) \end{pmatrix} = \begin{pmatrix} \tilde{h}(\theta_1) \\ \tilde{h}(\theta_2) \\ \vdots \\ \tilde{h}(\theta_N) \end{pmatrix}. \tag{4.37}$$

4.3.2 Non-flat graphene sheets

In this subsection, we introduce the discretization of (3.17) when Γ is a smooth open curve. Following the procedures in the last subsection, we first evaluate $\mathcal{S}$ and then discuss the evaluation of the operator $\mathcal{T}$.

Recall that from (3.14), we have

$$\mathcal{S}\psi(X(t)) = \int_{-1}^{1} \Phi(X(t), X(s))\ \psi(X(s))\ \frac{1}{\sqrt{1-s^2}} |X'(s)|\ ds.$$

For $t \in (-1,1)$, we do change of variable for $t = \cos\theta$. Define $\phi(\theta) = \psi(X(t))$, then $\mathcal{S}$ has the following form written in θ coordinate:

$$\mathcal{S}\phi(\theta) = \int_0^\pi \Phi(X(\cos\theta), X(\cos\theta'))\phi(\theta')|X'(\cos\theta')|\, d\theta' \tag{4.38}$$

According to [13], the kernel $\Phi(X(\cos\theta), X(\cos(\theta')))$ can be expanded as:

$$\begin{aligned}
\Phi(X(\cos\theta), X(\cos(\theta'))) &= \frac{i}{4}H_0^{(1)}\left(k|X(\cos\theta) - X(\cos\theta')|\right) \\
&= -\frac{1}{2\pi}J_0\left(k|X(\cos\theta) - X(\cos\theta')|\right)\cdot \ln|\cos\theta - \cos\theta'| \\
&\quad + \frac{i}{4}H_0^{(1)}\left(k|X(\cos\theta) - X(\cos\theta')|\right) \\
&\quad + \frac{1}{2\pi}J_0\left(k|X(\cos\theta) - X(\cos\theta')|\right)\cdot \ln|\cos\theta - \cos\theta'| \\
&=: M_1(\theta,\theta')\ln|\cos\theta - \cos\theta'| + M_2(\theta,\theta').
\end{aligned} \tag{4.39}$$

where $M_1(\theta,\theta') = -\frac{1}{2\pi}J_0\left(k|X(\cos\theta) - X(\cos\theta')|\right)$ and $M_2(\theta,\theta') = \Phi(X(\cos\theta), X(\cos(\theta'))) - M_1(\theta,\theta')\ln|\cos\theta - \cos\theta'|$. From the previous study, M_1 and M_2 are smooth functions of θ and θ' and the singular behavior of $\Phi(X(\cos\theta), X(\cos(\theta')))$ resides entirely in $\ln|\cos\theta - \cos\theta'|$.

From (4.38) and (4.39), we see that

$$\begin{aligned}
\mathcal{S}\phi(\theta) &= \int_0^\pi \left[M_1(\theta,\theta')\ln|\cos\theta - \cos\theta'| + M_2(\theta,\theta')\right]\phi(\theta')|X'(\cos\theta')|\, d\theta' \\
&= \int_0^\pi M_1(\theta,\theta')\ln|\cos\theta - \cos\theta'|\phi(\theta')|X'(\cos\theta')|\, d\theta' \\
&\quad + \int_0^\pi M_2(\theta,\theta')\phi(\theta')|X'(\cos\theta')|\, d\theta'
\end{aligned} \tag{4.40}$$

As before, $M_1(\theta,\theta')\phi(\theta')|X'(\cos\theta')|$ and $M_2(\theta,\theta')\phi(\theta')|X'(\cos\theta')|$ are approximated by the Chebyshev polynomial as a function of θ'. As such, from (4.23) and (4.24), we have

$$\begin{aligned}
\mathcal{S}\phi(\theta) &\approx \int_0^\pi \left[\sum_{j=1}^N M_1(\theta,\theta_j)\phi(\theta_j)|X'(\cos\theta_j)|L_j(\theta')\right]\ln|\cos\theta - \cos\theta'|\, d\theta' \\
&\quad + \int_0^\pi \sum_{j=1}^N M_2(\theta,\theta_j)\phi(\theta_j)|X'(\cos\theta_j)|L_j(\theta')\, d\theta'
\end{aligned}$$

$$= \sum_{j=1}^{N} \left[M_1(\theta,\theta_j)\phi(\theta_j)|X'(\cos\theta_j)|R_j(\theta) + \frac{\pi}{N} M_2(\theta,\theta_j)\phi(\theta_j)|X'(\cos\theta_j)| \right].$$

$$= \mathbf{S_g}(\theta) \begin{pmatrix} \phi(\theta_1) \\ \phi(\theta_2) \\ \vdots \\ \phi(\theta_N) \end{pmatrix}, \tag{4.41}$$

where

$$\mathbf{S_g}(\theta) = \begin{pmatrix} M_1(\theta,\theta_1)|X'(\cos\theta_1)|R_1(\theta) + \frac{\pi}{N} M_2(\theta,\theta_1)|X'(\cos\theta_1)| \\ M_1(\theta,\theta_2)|X'(\cos\theta_2)|R_2(\theta) + \frac{\pi}{N} M_2(\theta,\theta_2)|X'(\cos\theta_2)| \\ \vdots \\ M_1(\theta,\theta_N)|X'(\cos\theta_N)|R_N(\theta) + \frac{\pi}{N} M_2(\theta,\theta_N)|X'(\cos\theta_N)| \end{pmatrix}^{\mathrm{T}}.$$

In the following, we evaluate the operator $\mathcal{T}$. Recall from (3.15),

$$\mathcal{T}\psi(X(t)) = \int_{-1}^{1} \frac{\partial^2\Phi(X(t),X(s))}{\partial\nu_{X(t)}\partial\nu_{X(s)}}\, \psi(X(s))\, \sqrt{1-s^2}|X'(s)|\, ds.$$

Changing the variable $t = \cos\theta$ gives

$$(\mathcal{T}\phi)(\theta) = \int_0^{\pi} \frac{\partial^2\Phi(X(\cos\theta),X(\cos\theta'))}{\partial\nu_{X(\cos\theta)}\, \partial\nu_{X(\cos\theta')}} \phi(\theta')|X'(\cos\theta')| \sin^2\theta'\, d\theta'. \tag{4.42}$$

Since we do not have an effective way to handle the kernel $\dfrac{\partial^2\Phi(X(\cos\theta),X(\cos\theta'))}{\partial\nu_{X(\cos\theta)}\, \partial\nu_{X(\cos\theta')}}$, the same technique to decompose $\mathcal{T}$ is applied here:

$$\mathcal{T}\psi = \mathcal{T}^g\psi + \mathcal{T}^s\psi, \tag{4.43}$$

where

$$\mathcal{T}^g\psi(X(t)) \;=\; k^2 \int_{-1}^{1} \Phi(X(t),X(s))\psi(X(s))|X'(s))|\sqrt{1-s^2}\; \nu_{X(t)}\cdot\nu_{X(s)}\, ds,$$

$$\mathcal{T}^s\psi(X(t)) \;=\; \frac{1}{|X'(t)|}\frac{d}{dt}\int_{-1}^{1}\Phi(X(t),X(s))\frac{d}{ds}\left(\psi(X(s))\sqrt{1-s^2}\right)\,ds.$$

These operators can be expressed in terms of the θ coordinate as

$$\mathcal{T}^g\phi(\theta) \;=\; k^2\int_0^{\pi}\Phi(X(\cos\theta),X(\cos\theta'))\phi(\theta')|X'(\cos\theta'))|\sin^2(\theta')\;\nu_{X(\cos\theta)}\cdot\nu_{X(\cos\theta')}\;d\theta', \tag{4.44}$$

$$\mathcal{T}^s\phi(\theta) \;=\; \frac{1}{|X'(\cos\theta)|}\cdot\frac{1}{\sin\theta}\cdot\frac{d}{d\theta}\int_0^{\pi}\Phi(X(\cos\theta),X(\cos\theta'))\frac{d}{d\theta'}\left(\phi(\theta')\sin\theta'\right)\;d\theta' \tag{4.45}$$

From (4.38) and (4.44), it is seen that $\mathcal{T}^g\phi(\theta)$ differs from $\mathcal{S}\phi(\theta)$ by $\sin^2(\theta')\;\nu_{X(\cos\theta)}\cdot\nu_{X(\cos\theta')}$ inside the integral. In light of (4.23) and (4.24), we have

$$\begin{aligned}\mathcal{T}^g\phi(\theta) \;&\approx\; k^2\sum_{j=1}^{N}R_j(\theta)M_1(\theta,\theta_j)\phi(\theta_j)|X'(\cos\theta_j)|\sin^2(\theta_j)\;\nu_{X(\cos\theta)}\cdot\nu_{X(\cos\theta_j)}\\ &\quad+\frac{k^2\pi}{N}\sum_{j=1}^{N}M_2(\theta,\theta_j)\phi(\theta_j)|X'(\cos\theta_j)|\sin^2(\theta_j)\;\nu_{X(\cos\theta)}\cdot\nu_{X(\cos\theta_j)}\\ &=\; \mathbf{T_{gg}}(\theta)\begin{pmatrix}\phi(\theta_1)\\ \phi(\theta_2)\\ \vdots\\ \phi(\theta_N)\end{pmatrix},\end{aligned} \tag{4.46}$$

where

$$\mathbf{T_{gg}}(\theta)=k^2\begin{pmatrix}|X'(\cos\theta_1)|\sin^2\theta_1\;\nu_{X(\cos\theta)}\cdot\nu_{X(\cos\theta_1)}\left[M_1(\theta,\theta_1)R_1(\theta)+\frac{\pi}{N}M_2(\theta,\theta_1)\right]\\ |X'(\cos\theta_2)|\sin^2\theta_2\;\nu_{X(\cos\theta)}\cdot\nu_{X(\cos\theta_2)}\left[M_1(\theta,\theta_2)R_2(\theta)+\frac{\pi}{N}M_2(\theta,\theta_2)\right]\\ \vdots\\ |X'(\cos\theta_N)|\sin^2\theta_N\;\nu_{X(\cos\theta)}\cdot\nu_{X(\cos\theta_N)}\left[M_1(\theta,\theta_N)R_N(\theta)+\frac{\pi}{N}M_2(\theta,\theta_N)\right]\end{pmatrix}^{\mathbf{T}}.$$

From (4.45), it is clear that $\mathcal{T}^s$ can be viewed as the composition of three operators:

$$\mathcal{T}^s\phi=\left(\mathcal{T}_{1g}\cdot\mathcal{T}_{2g}\cdot\mathcal{T}_{3g}\right)\phi.$$

where

$$\mathcal{T}_{1g}f(\theta) = \frac{1}{|X'(\cos\theta)|}\frac{1}{\sin\theta}\frac{df(\theta)}{d\theta} = \frac{1}{|X'(t)|}\cdot\left(-\frac{d\tilde{f}(t)}{dt}\right) \text{ with } \tilde{f}(t) = f(\theta); \tag{4.47}$$

$$\mathcal{T}_{2g}f = \int_0^\pi \Phi(X(\cos\theta), X(\cos\theta'))f(\theta')\, d\theta'; \tag{4.48}$$

$$\mathcal{T}_{3g}f = \frac{d}{d\theta}\left(f(\theta)\sin\theta\right). \tag{4.49}$$

We can evaluate $\mathcal{T}_{1g}$,$\mathcal{T}_{2g}$ and $\mathcal{T}_{3g}$ in a similar way as the case of line segment.

For $\mathcal{T}_{1g}$, by (4.32),

$$\begin{aligned}\mathcal{T}_{1g} &\approx -\frac{2}{N}\frac{1}{|X'(\cos\theta)|}\mathbf{T_{1Lb}}(\theta)PB\begin{pmatrix} f(\theta_1)\\ f(\theta_2)\\ \vdots\\ f(\theta_N)\end{pmatrix}\\ &= \mathbf{T_{1gb}}(\theta)\begin{pmatrix} f(\theta_1)\\ f(\theta_2)\\ \vdots\\ f(\theta_N)\end{pmatrix},\end{aligned} \tag{4.50}$$

where

$$\mathbf{T_{1gb}}(\theta) = -\frac{2}{N}\frac{1}{|X'(\cos\theta)|}\mathbf{T_{1Lb}}(\theta)PB.$$

For $\mathcal{T}_2$, we apply the idea of evaluating $\mathcal{S}\phi$, by (4.41), it is easy to deduce that

$$\begin{aligned}\mathcal{T}_{2g}f(\theta) &\approx \sum_{j=1}^{N}\left[M_1(\theta,\theta_j)f(\theta_j)R_j(\theta) + \frac{\pi}{N}M_2(\theta,\theta_j)f(\theta_j)\right]\\ &= \mathbf{T_{2g}}(\theta)\begin{pmatrix} f(\theta_1)\\ f(\theta_2)\\ \vdots\\ f(\theta_N)\end{pmatrix},\end{aligned} \tag{4.51}$$

where

$$\mathbf{T_{2g}}(\theta) = \begin{pmatrix} M_1(\theta,\theta_1)R_1(\theta) + \dfrac{\pi}{N}M_2(\theta,\theta_1) \\ M_1(\theta,\theta_2)R_2(\theta) + \dfrac{\pi}{N}M_2(\theta,\theta_2) \\ \vdots \\ M_1(\theta,\theta_N)R_N(\theta) + \dfrac{\pi}{N}M_2(\theta,\theta_N) \end{pmatrix}^{\mathrm{T}}.$$

Note that $\mathcal{T}_{3g}$ is the same as the one for the line segment case. Thus its discretization also leads to (4.33).

In summary, from (4.50), (4.51) and (4.33), the evaluation of $\mathcal{T}^s\phi$ is given by

$$\begin{aligned}
\mathcal{T}^s\phi(\theta) &= (\mathcal{T}_{1g}\cdot\mathcal{T}_{2g}\cdot\mathcal{T}_{3g})\,\phi(\theta) \\
&\approx \mathbf{T_{1gb}}(\theta)\begin{pmatrix} (\mathcal{T}_{2g}\cdot\mathcal{T}_{3g})\phi(\theta_1) \\ (\mathcal{T}_{2g}\cdot\mathcal{T}_{3g})\phi(\theta_2) \\ \vdots \\ (\mathcal{T}_{2g}\cdot\mathcal{T}_{3g})\phi(\theta_N) \end{pmatrix} \\
&\approx \mathbf{T_{1gb}}(\theta)\begin{pmatrix} \mathbf{T_{2g}}(\theta_1) \\ \mathbf{T_{2g}}(\theta_2) \\ \vdots \\ \mathbf{T_{2g}}(\theta_N) \end{pmatrix}\begin{pmatrix} \mathcal{T}_{3g}\phi(\theta_1) \\ \mathcal{T}_{3g}\phi(\theta_2) \\ \vdots \\ \mathcal{T}_{3g}\phi(\theta_N) \end{pmatrix} \\
&\approx \frac{1}{2}\mathbf{T_{1gb}}(\theta)\begin{pmatrix} \mathbf{T_{2g}}(\theta_1) \\ \mathbf{T_{2g}}(\theta_2) \\ \vdots \\ \mathbf{T_{2g}}(\theta_N) \end{pmatrix}\begin{pmatrix} \mathbf{T_{2Lb}}(\theta_1) \\ \mathbf{T_{2Lb}}(\theta_2) \\ \vdots \\ \mathbf{T_{2Lb}}(\theta_N) \end{pmatrix} B\begin{pmatrix} \phi(\theta_1) \\ \phi(\theta_2) \\ \vdots \\ \phi(\theta_N) \end{pmatrix} \\
&= \mathbf{T_{sg}}(\theta)\begin{pmatrix} \phi(\theta_1) \\ \phi(\theta_2) \\ \vdots \\ \phi(\theta_N) \end{pmatrix},
\end{aligned} \tag{4.52}$$

where

$$\mathbf{T_{sg}}(\theta) = \frac{1}{2}\mathbf{T_{1gb}}(\theta) \begin{pmatrix} \mathbf{T_{2g}}(\theta_1) \\ \mathbf{T_{2g}}(\theta_2) \\ \vdots \\ \mathbf{T_{2g}}(\theta_N) \end{pmatrix} \begin{pmatrix} \mathbf{T_{2Lb}}(\theta_1) \\ \mathbf{T_{2Lb}}(\theta_2) \\ \vdots \\ \mathbf{T_{2Lb}}(\theta_N) \end{pmatrix} B.$$

We recall our boundary integral equation from (3.17) again:

$$\mathcal{A}\phi(\theta) = \left[\sin\theta\, \mathcal{S} - \frac{i\tau}{k}\mathcal{T}\mathcal{S}\right] \phi(\theta) = \tilde{h}(\theta).$$

Combining (4.41), (4.46) and (4.52), it follows that

$$\begin{aligned} \mathcal{T}\mathcal{S}\phi(\theta) &= (\mathcal{T}^g + \mathcal{T}^s)(\mathcal{S}\phi(\theta)) \\ &\approx [\mathbf{T_{gg}}(\theta) + \mathbf{T_{sg}}(\theta)] \begin{pmatrix} \mathcal{S}\phi(\theta_1) \\ \mathcal{S}\phi(\theta_2) \\ \vdots \\ \mathcal{S}\phi(\theta_N) \end{pmatrix} \\ &\approx [\mathbf{T_{gg}}(\theta) + \mathbf{T_{sg}}(\theta)] \begin{pmatrix} \mathbf{S_g}(\theta_1) \\ \mathbf{S_g}(\theta_2) \\ \vdots \\ \mathbf{S_g}(\theta_N) \end{pmatrix} \begin{pmatrix} \phi(\theta_1) \\ \phi(\theta_2) \\ \vdots \\ \phi(\theta_N) \end{pmatrix} \\ &= \mathbf{TS_g}(\theta) \begin{pmatrix} \phi(\theta_1) \\ \phi(\theta_2) \\ \vdots \\ \phi(\theta_N) \end{pmatrix}, \end{aligned} \tag{4.53}$$

where

$$\mathbf{TS_g}(\theta) = [\mathbf{T_{gg}}(\theta) + \mathbf{T_{sg}}(\theta)] \begin{pmatrix} \mathbf{S_g}(\theta_1) \\ \mathbf{S_g}(\theta_2) \\ \vdots \\ \mathbf{S_g}(\theta_N) \end{pmatrix}.$$

Therefore, the discretization of the integral equation (3.17) yields

$$\left[\sin\theta \mathbf{S_g}(\theta) - \frac{i\tau}{k}\mathbf{T}\mathbf{S_g}(\theta)\right] \begin{pmatrix} \phi(\theta_1) \\ \phi(\theta_2) \\ \vdots \\ \phi(\theta_N) \end{pmatrix} = \tilde{h}(\theta). \tag{4.54}$$

By choosing the collocation points at Chebyshev points θ_j for the above equation, it leads to the following linear system with the unknown $\phi(\theta_j)$:

$$\begin{pmatrix} \sin\theta_1 \mathbf{S_g}(\theta_1) - \frac{i\tau}{k}\mathbf{T}\mathbf{S_g}(\theta_1) \\ \sin\theta_2 \mathbf{S_g}(\theta_2) - \frac{i\tau}{k}\mathbf{T}\mathbf{S_g}(\theta_2) \\ \vdots \\ \sin\theta_N \mathbf{S_g}(\theta_N) - \frac{i\tau}{k}\mathbf{T}\mathbf{S_g}(\theta_N) \end{pmatrix} \begin{pmatrix} \phi(\theta_1) \\ \phi(\theta_2) \\ \vdots \\ \phi(\theta_N) \end{pmatrix} = \begin{pmatrix} \tilde{h}(\theta_1) \\ \tilde{h}(\theta_2) \\ \vdots \\ \tilde{h}(\theta_N) \end{pmatrix}. \tag{4.55}$$

We have completed the discretization of boundary integral equation from (3.17) using the Nystrom method. The solution of the linear system will be accomplished by iterative methods. This will be discussed in next chapter.

Chapter 5

Iterative solvers for linear system

In this chapter we introduce iterative methods for solving the linear system obtained from Nystrom discretization. In particular, we introduce generalized minimum residual (GMRES) and biconjugate gradient method (BCG) (see [54] for detailed description of the two methods).

5.1 Introduction

There are two main classes of iterative methods to solve the system of linear equations : stationary iterative methods and Krylov subspace methods. Stationary iterative methods are so named because solving the linear systems is the process of finding the stationary point of a contraction operator. In detail, to solve $Ax = b$, we split A as $A = B - C$ where B is nonsingular. Then we can write the linear system as:

$$Bx = Cx + b,$$

or equivalently,

$$x = B^{-1}(Cx + b).$$

This leads to the fixed point iteration:

$$x^{(n+1)} = B^{-1}(Cx^{(n)} + b) = x^{(n)} + B^{-1}(b - Ax^{(n)}).$$

These methods are easy to derive and implement, but convergence is guaranteed only for a limited class of A for which there exist B and C, such that $A = B - C$ and $||B^{-1}C|| < 1$ under certain norm. Therefore, the stationary iterative methods are largely supplanted by

more sophisticated methods such as Krylov subspace methods nowadays. The idea of Krylov subspace method is to project a high-dimensional problem into a lower-dimensional Krylov subspace.

In the following, we briefly introduce the Krylov subspace methods and then discuss GMRES and BCG in detail. Now we define the Krylov subspace as follows.

Definition 5.1 *Given a nonsingular matrix $A \in \mathbb{C}^{m\times m}$ and $b \neq \mathbf{0} \in \mathbb{C}^m$, the nth Krylov subspace $\mathcal{K}_n(A, b)$ generated by A and b is*

$$\mathcal{K}_n := \mathcal{K}_n(A, b) := \textit{span}\left\langle b, Ab, \cdots, A^{n-1}b\right\rangle.$$

Starting with a initial guess x_0 and corresponding residual $\mathbf{r}_0 = b - Ax_0$, the Krylov subspace method is an iterative method to generate a sequence of x_n such that

$$x_n - x_0 \in \mathcal{K}_n(A, \mathbf{r}_0)$$

with certain optimality property. The process continues until finding the exact solution or to the desired accuracy.

There are three popular methods in the family of Krylov subspace methods: generalized minimum residual (GMRES), biconjugate gradient method (BCG) and conjugate gradient method(CG). CG is applied when matrix A is symmetric and positive definite, while GMRES and BCG are two popular methods to solve linear system with general matrices.

5.2 Generalized minimum residual (GMRES)

In this section, we introduce the Arnoldi iteration and illustrate how it can be used to solve linear system $Ax = b,\ A \in \mathbb{C}^{m\times m}$, which is known as GMRES.

The Arnoldi iteration is used to reduce A to the Hessenberg form by an orthogonal similarity transformation, which can be written as $A = QHQ^*$ or $AQ = QH$. Similar to the Gram-Schmidt method, it has the advantage that it can be stopped part-way, leaving one with

a partial reduction to the Hessenberg form that is exploited to form iterative algorithms for systems of equations.

Computing the full reduction is impractical when m is large. Instead, the Arnoldi iteration considers the first n columns of $AQ = QH$. Let Q_n be the $m \times n$ matrix whose columns are the first n columns of Q:

$$Q_n = \left(\begin{array}{c|c|c|c} q_1 & q_2 & \cdots & q_n \end{array} \right).$$

Let H_n be the $(n+1) \times n$ upper-left section of H:

$$H_n = \begin{pmatrix} h_{11} & h_{12} & \cdots & h_{1n} \\ h_{21} & h_{22} & & h_{2n} \\ & \ddots & \ddots & \vdots \\ & & h_{n,n-1} & h_{nn} \\ & & & h_{n+1,n} \end{pmatrix}$$

It is seen that H_n is also a Hessenberg matrix. Then we have

$$AQ_n = Q_{n+1}H_n,$$

that is

$$A \left(\begin{array}{c|c|c|c} q_1 & q_2 & \cdots & q_n \end{array} \right) = \left(\begin{array}{c|c|c|c} q_1 & q_2 & \cdots & q_{n+1} \end{array} \right) \begin{pmatrix} h_{11} & h_{12} & \cdots & h_{1n} \\ h_{21} & h_{22} & & h_{2n} \\ & \ddots & \ddots & \vdots \\ & & h_{n,n-1} & h_{nn} \\ & & & h_{n+1,n} \end{pmatrix} \tag{5.1}$$

We can write the nth column of the above equation explicitly as:

$$Aq_n = h_{1n}q_1 + \cdots + h_{nn}q_n + h_{n+1,n}q_{n+1}. \tag{5.2}$$

The Arnoldi iteration starts from an arbitrary b with $q_1 = \dfrac{b}{||b||}$. Then at step n, we use the $(n+1)$ term recurrence relation determined by (5.2) ,

for $n = 1, 2, 3, \cdots$

$v = Aq_n$,

for $j = 1 : n$

$h_{jn} = q_j^* v$

$v = v - h_{jn} q_j$

$h_{n+1,n} = ||v||$

$q_{n+1} = \dfrac{v}{h_{n+1,n}}$

It is clear that span $\langle b, Ab, \cdots, A^{n-1}b \rangle = \mathcal{K}_n =$ span $\langle q_1, q_2, \cdots, q_n \rangle$.

The idea of GMRES is to generate a sequence of x_n to approximate the exact solution of $Ax = b$, at step n, finding $x_n \in \mathcal{K}_n$ that minimizes the norm of the residual $r_n = b - Ax_n$. It implies that at each step, x_n is determined by solving a least squares problem. To be more precise, at each step, the least squares problem is to find a $y \in \mathbb{C}^n$ with $x_n = Q_n y$ such that

$$||AQ_n y - b|| \text{ is minimized.} \tag{5.3}$$

By Arnoldi iteration, the above problem can be transformed to

$$||Q_{n+1} H_n y - b|| \text{ is minimized.} \tag{5.4}$$

We note that by multiplying Q_{n+1}^* on the left, (5.4) does not change the norm. Furthermore, $Q_{n+1}^* b = ||b|| e_1$. Therefore, the final form of the GMRES least squares problem is:

$$||H_n y - ||b|| e_1|| \text{ is minimized.} \tag{5.5}$$

The GMRES algorithm can be summarized as follows:

$q_1 = \dfrac{b}{||b||}$

for $n = 1, 2, 3, \cdots$

step n of Arnoldi iteration

Find y to minimize $||H_n y - ||b||e_1||$

$x_n = Q_n y$.

The least squares problem can be solved via QR factorization in the usual way.

5.3 Biconjugate gradient method (BCG)

From last section, it is known that GMRES retains orthogonality of the residuals and has the effect of minimization. However, it is at the cost of large storage demand with a growing recurrence length from Arnoldi iteration. Hence it is natural to seek methods with short recurrence relations. The biconjugate gradient method (BCG) is a popular method in this class. It is difficult to say which method is better between the GRMRES and BCG. Therefore, in this section, we briefly introduce the idea of BCG.

If A is hermitian, then the Hessenberg matrix H_n from the Arnoldi iteration is in fact tridiagonal, thus instead of $(n+1)$-term recurrence at step n, the new iteration involves just a three-term recurrence. However, when A is not hermitian, if we insist on a tridiagonal result, we have to give up the use of unitary transformations.

It is known that for general $A \in \mathbb{C}^{m\times m}$, there exists a nonsingular but not generally unitary matrix V such that $AV = VT$, where T is tridiagonal. Define $W = V^{-*}$, then $A^*W = WT^*$. Let v_j and w_j be the j th columns of V and W, these vectors are biorthogonal in the sense that

$$w_j^* v_j = \delta_{ij}.$$

From $AV = VT$ and $A^*W = WT^*$ and since T and T^* are tridiagonal, we have

$$A\left(\begin{array}{c|c|c} v_1 & \cdots & v_n \end{array} \right) = \left(\begin{array}{c|c|c} v_1 & \cdots & v_{n+1} \end{array} \right) \begin{pmatrix} a_1 & r_1 & & & \\ b_1 & a_2 & r_2 & & \\ & b_2 & a_3 & \ddots & \\ & & \ddots & \ddots & r_{n-1} \\ & & & b_{n-1} & a_n \\ & & & & b_n \end{pmatrix} \tag{5.6}$$

which leads to the three-term recurrence relation:

$$Av_n = r_{n-1}v_{n-1} + a_n v_n + b_n v_{n+1}. \tag{5.7}$$

The similar form holds as follows:

$$A^*\left(\begin{array}{c|c|c} w_1 & \cdots & w_n \end{array} \right) = \left(\begin{array}{c|c|c} w_1 & \cdots & w_{n+1} \end{array} \right) \begin{pmatrix} \overline{a_1} & \overline{b_1} & & & \\ \overline{r_1} & \overline{a_2} & \overline{b_2} & & \\ & \overline{r_2} & \overline{a_3} & \ddots & \\ & & \ddots & \ddots & \overline{b_{n-1}} \\ & & & \overline{r_{n-1}} & \overline{a_n} \\ & & & & \overline{r_n} \end{pmatrix} \tag{5.8}$$

with

$$A^*w_n = \overline{b_{n-1}}w_{n-1} + \overline{a_n}w_n + \overline{r_n}w_{n+1}. \tag{5.9}$$

It is clear that $v_n \in \mathcal{K}_n(A, v_1)$ and $w_n \in \mathcal{K}_n(A^*, w_1)$.

Take $v_1 = b$ and $w_1 = v_1/||v_1||_2$. The basic idea of BCG is to pick a sequence $x_n \in \mathcal{K}_n(A, b)$ with the residual $r_n = Ax_n - b$ orthogonal to the Krylov space $\mathcal{K}_n(A^*, w_1)$, where v_n and w_n are defined by (5.7) and (5.9). Unlike GMRES, $||r_n||_2$ is not minimized at each step while we take the advantage of short recurrence from (5.7) and (5.9).

Chapter 6

Numerical examples

In this chapter, we carry out extensive numerical studies to demonstrate the effectiveness of the proposed boundary integral equation solver for the simulation of graphene plasmons. The numerical results presented below are implemented in Matlab. In Section 6.1, we compare the efficiency of the regularized integral equation formulation with the non-regularized version. In Section 6.2 and 6.3, we perform computational simulations of graphene plasmon for various setups. Both flat graphene sheet and non-flat ones will be considered.

6.1 Efficiency of the well-conditioned boundary integral equation solver

We choose the cross-section of the graphene sheet to be $\Gamma = [-\pi, \pi]$. The parameter τ, which is defined in (3.11), is chosen as 0.2. We consider the scattering by a normal incident plane wave $u^i = e^{-iky}$ with the wavenumber $k = 1$. GMRES is applied to solve the discretized linear system (4.37). Table 6.1 shows the number of iterations when the regularized integral formulation (3.17) and the unregularized integral formulation (3.12) are used for various N. The tolerance for both formulations is 10^{-8}.

Table 6.1: Iteration numbers for regularized and unregularized integral formulations.

N	400	800	1600	3200
Regularized formulation	65	67	68	68
Unregularized formulation	211	302	430	610

It is clear that solving the regularized formulation requires fewer iterations compared to the unregularized formulation for all N. More precisely, as N doubles, the iteration number for the

regularized formula remains almost the same, while the iteration number for the unregularized formulation increases by approximately 50%.

6.2 Scattering by flat graphene sheets

In this section, we present four examples when the cross-section of graphene sheet is given by a line segment $[-\pi, \pi]$. Both normal and oblique incidences are investigated.

Example 1 We consider the normal incidence with the incidence angle $\theta = 0$. That is, the plane wave $u^i = e^{-iky}$. We discretize the integral formulation with $N = 800$. Figures 6.1 and 6.3 plot the normal derivative $\dfrac{\partial u}{\partial y}$ along Γ for the wavenumber $k = 1$ and $k = 2$, respectively. Figures 6.2 and 6.3 demonstrate the corresponding scattered field near the graphene sheet. It is observed that the surface plasmon occurs along Γ. More precisely, the scattered wave u^s is much more oscillatory than the incident wave along Γ, and the energy for the plasmon wave is localized near the interface Γ. For comparison, in Figure 6.5 and 6.6, we demonstrate the scattered wave for $k = 1$ and $k = 2$ when a perfect conductor sheet, instead of a graphene sheet, is sitting in the vacuum. For the latter setup, it is known that no plasmon occurs.

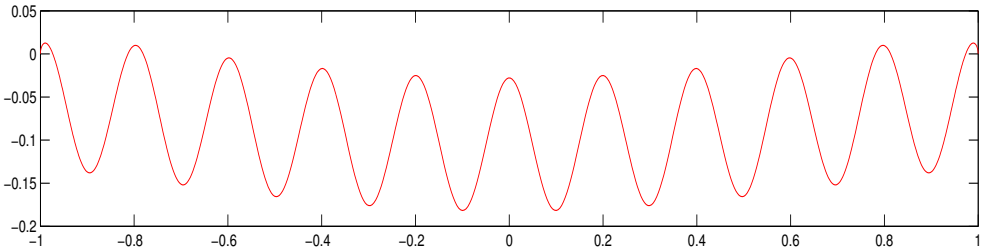

Figure 6.1: The normal derivative $\dfrac{\partial u}{\partial y}$ along Γ. $k = 1$.

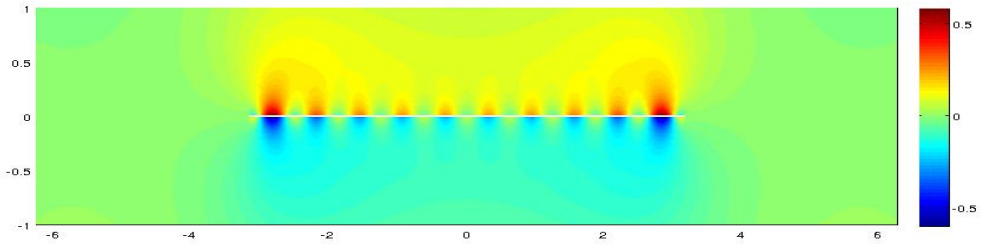

Figure 6.2: The scattered field u^s near the graphene sheet. $k = 1$.

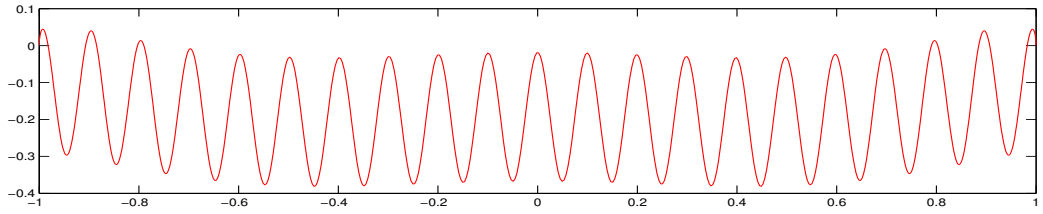

Figure 6.3: The normal derivative $\dfrac{\partial u}{\partial y}$ along Γ. $k = 2$.

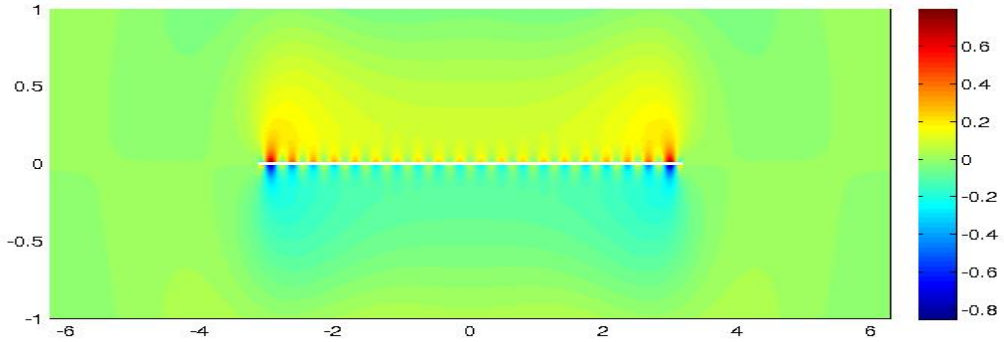

Figure 6.4: he scattered field u^s near the graphene sheet. $k = 2$.

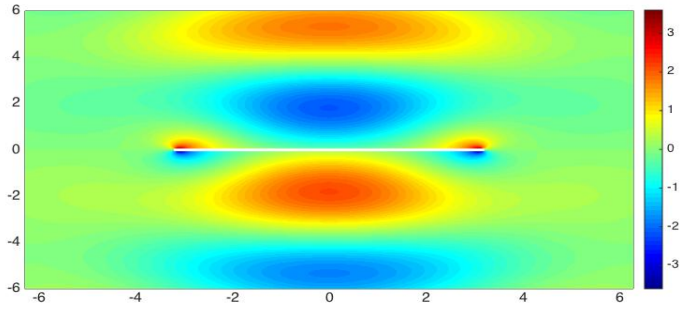

Figure 6.5: The scattered field u^s if Γ is a perfect conductor. The boundary condition is $\dfrac{\partial u}{\partial y} = 0$ on Γ. $k = 1$.

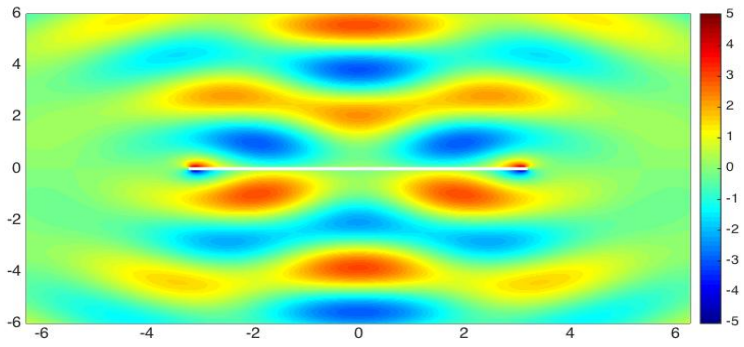

Figure 6.6: The scattered field u^s if Γ is a perfect conductor. The boundary condition is $\dfrac{\partial u}{\partial y} = 0$ on Γ. $k = 2$.

Example 2 In this example, we test the scattering by an oblique incident wave instead of a normal incident wave. The incidence angle $\theta = \pi/6$ such that the plane wave $u^i = e^{ik(1/2x - \sqrt{3}/2y)}$. We also discretize the integral equation with $N = 800$. Figures 6.7 and 6.9 show the normal derivative $\dfrac{\partial u}{\partial y}$ along Γ for the wavenumber $k = 1$ and $k = 2$, respectively. Figures 6.8 and 6.10 plot the corresponding scattered field near the graphene sheet. As seen from Figures 6.8 and 6.10, the plasmon also occurs along Γ and the scattered wave is highly oscillatory.

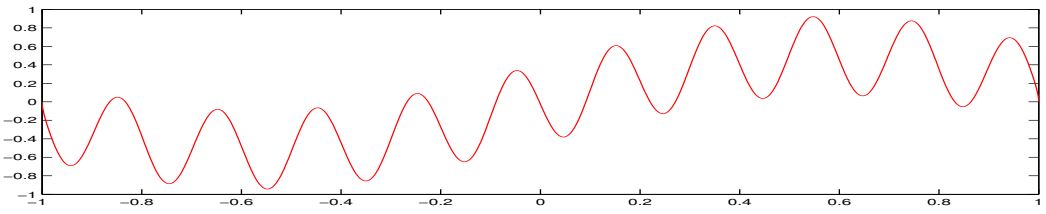

Figure 6.7: The normal derivative $\dfrac{\partial u}{\partial y}$ along Γ. $k = 1$.

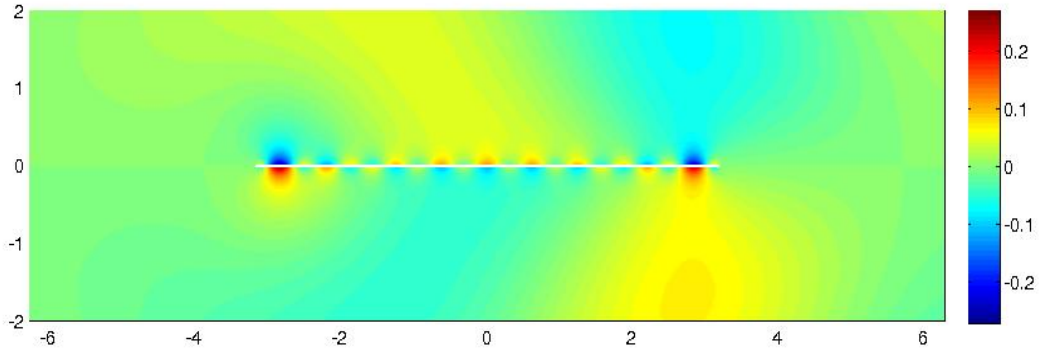

Figure 6.8: The scattered field u^s near Γ. $k = 1$.

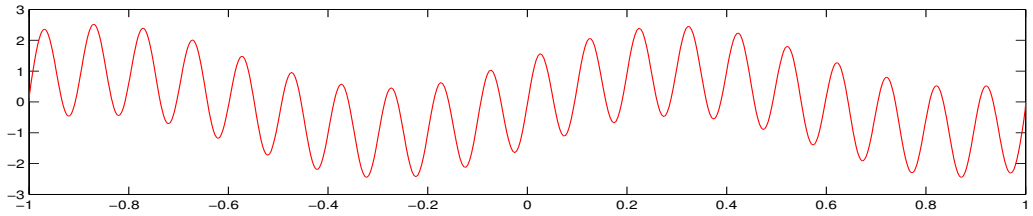

Figure 6.9: The normal derivative $\dfrac{\partial u}{\partial y}$ along Γ. $k = 2$.

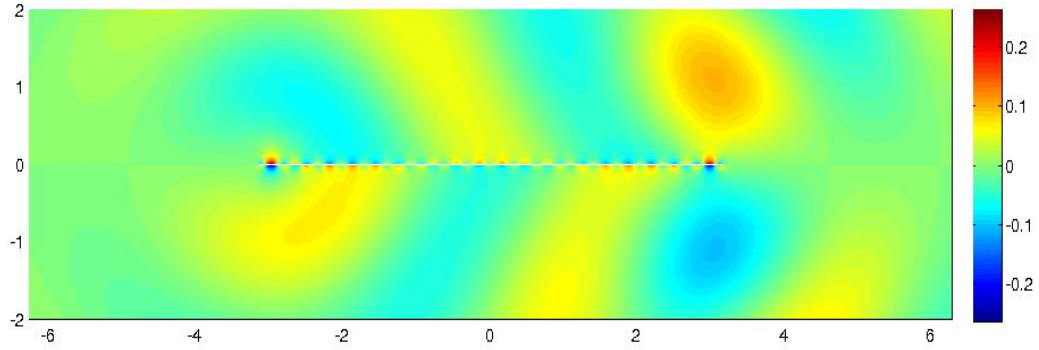

Figure 6.10: The scattered field u^s near Γ. $k = 2$.

6.3 Scattering by non-flat graphene sheets

In this section, the graphene sheet is assumed to be non-flat. We choose the parameterization of Γ with $x = Lt$, $y = H\sin(Lt)$, where $t \in [-1, 1]$. The constants L and H are given by $L = \pi$, $H = 0.2$. The wavenumber is set as $k = 1$. We use $N = 800$ to discretize the integral equation.

Example 1 We consider both the normal incidence and the oblique incidence with incidence angle $\theta = \pi/6$. The normal derivative $\dfrac{\partial u}{\partial y}$ along Γ for both cases are shown in Figure 6.11 and 6.12, respectively. Figure 6.13 and 6.14 clearly demonstrates the oscillatory behavior of scattered field along Γ. In addition, these wave modes are localized along Γ. The difference in Figure 6.1 (6.3) and Figure 6.11 (6.12) also reflects the difference of the scattering by flat and non-flat graphene sheet.

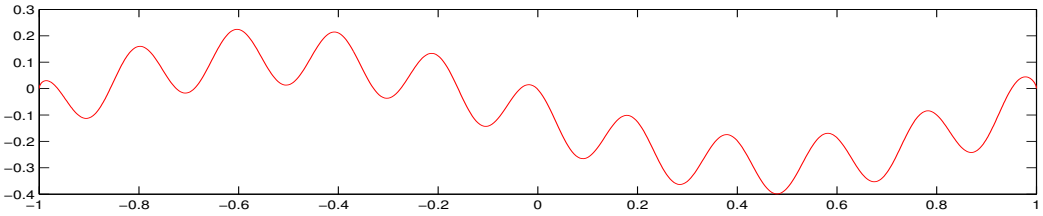

Figure 6.11: The normal derivative $\dfrac{\partial u}{\partial y}$ along Γ for the normal incidence.

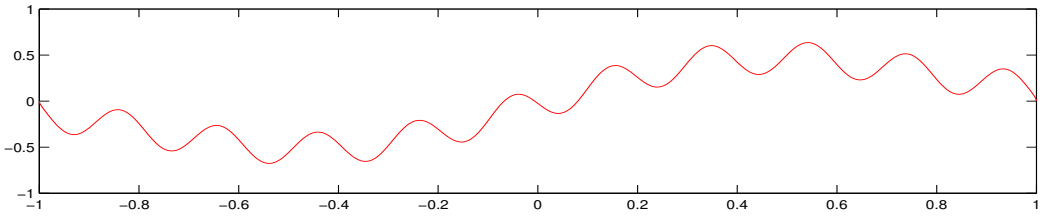

Figure 6.12: The normal derivative $\dfrac{\partial u}{\partial y}$ along Γ for the oblique incidence.

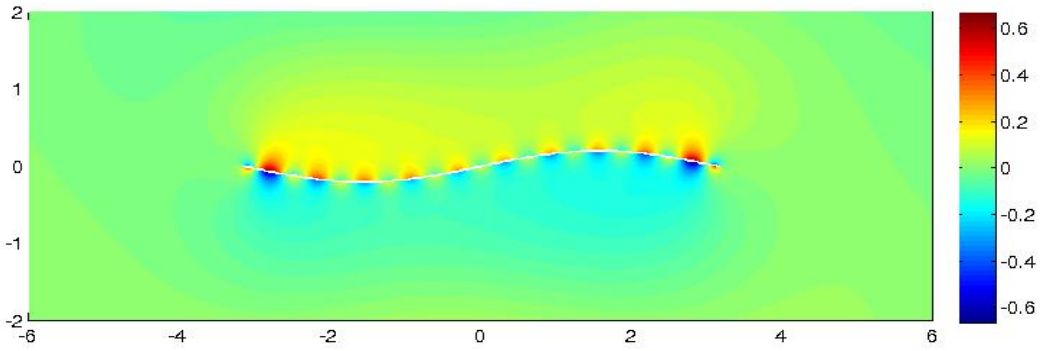

Figure 6.13: The scattered field u^s near the graphene sheet.

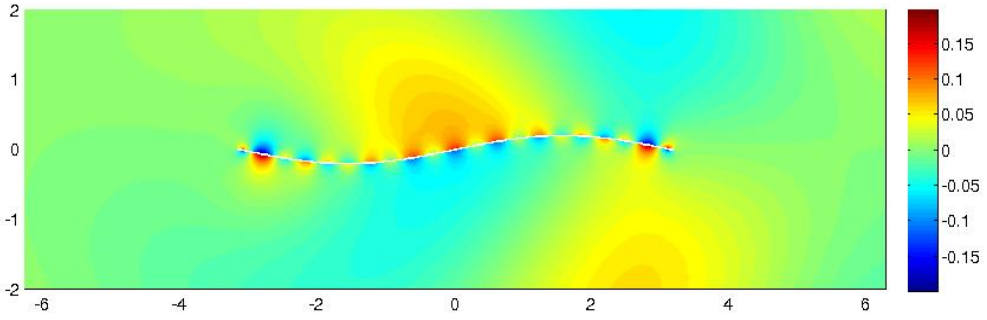

Figure 6.14: The scattered field u^s near the graphene sheet.

Chapter 7

Error estimation

In this chapter, we derive the error estimate for the Nystrom discretization method used for the discretization of the well-conditioned integral equation. We first present some preliminaries in Section 7.1. The error estimation for the numerical approximation of the integral operators is derived in Section 7.2, and the error estimation for the solution of the integral equation is given in Section 7.3.

7.1 Preliminaries

For functions on $[-1, 1]$, we define the inner product with weight $1/\sqrt{1-x^2}$:

$$\langle f(x), g(x) \rangle = \int_{-1}^{1} \frac{f(x)g(x)}{\sqrt{1-x^2}}\, dx.$$

From (4.2) in Section 4.1, we know that Chebyshev polynomials $\{T_n, n = 0, 1, \cdots\}$ forms an orthogonal polynomial system under this inner product. We define the norms with the above inner product as follows:

$$||f||_0^2 = \langle f, f \rangle, \qquad ||f||_s^2 = \sum_{i=0}^{s} ||f^{(i)}||_0^2. \tag{7.1}$$

Let W_T^s be a function space equipped with the above norm such that

$$W_T^s = \{f(x) \Big| ||f(x)||_s^2 < +\infty\}.$$

Throughout this chapter, we denote the Chebyshev polynomial interpolant with degree N of f by $I_N(f)$. The following theorem presents an error estimate for the Chebyshev polynomial interpolation as stated in [53].

Theorem 7.1 *(Interpolation Error) Assume $v(x)$ is in W_T^r with $r > \frac{1}{2}$. Then for any real σ, $0 \leq 2\sigma \leq r$, it holds that*

$$||v - I_N(v)||_\sigma \leq C \left(\frac{1}{N}\right)^{r-2\sigma} ||v||_r. \tag{7.2}$$

The following lemma follows from the expansion of a smooth function by Chebyshev polynomials.

Lemma 7.1 *Let $\{T_n(t)\}_{n=0}^\infty$ be the Chebyshev polynimials on $[-1,1]$. If $M(t,s) \in C^\infty[-1,1] \times C^\infty[-1,1]$, then $M(t,s)$ can be expanded as*

$$M(t,s) = \sum_{n=0}^{\infty} c_n(t) T_n(s), \quad \textit{where} \quad c_n(t) = \langle M(t,\cdot), T_n(\cdot) \rangle . \tag{7.3}$$

Moreover, $\dfrac{\partial^i}{\partial t^i} \dfrac{\partial^j}{\partial s^j} M(t,s) = \sum_{n=0}^\infty c_n^{(i)}(t) T_n^{(j)}(s)$.

7.2 Error estimation for the numerical approximation of the integral operators

In this section, we present an error estimate for the numerical approximation of operators $\mathcal{S}$ and $\mathcal{T}$.

Let $\varphi(t) = \psi(X(t))$. Recall from (3.14) and (4.39), we have

$$\begin{aligned}
(\mathcal{S}\varphi)(t) &= \int_{-1}^{1} \Phi(X(t), X(s))\ \varphi(s)\ \frac{1}{\sqrt{1-s^2}} |X'(s)|\ ds \\
&= \int_{-1}^{1} \left[M_1(t,s) \ln|t-s| + M_2(t,s)\right] \varphi(s) \frac{|X'(s)|}{\sqrt{1-s^2}}\ ds \\
&= \int_{-1}^{1} \ln|t-s| M_1(t,s) \varphi(s) \frac{|X'(s)|}{\sqrt{1-s^2}}\ ds + \int_{-1}^{1} M_2(t,s) \varphi(s) \frac{|X'(s)|}{\sqrt{1-s^2}}\ ds.
\end{aligned} \tag{7.4}$$

The Nystrom discretization for $\mathcal{S}\varphi$ leads to $\mathcal{S}_N\varphi$, which is given by

$$\mathcal{S}_N\varphi(t) = \int_{-1}^{1} \ln|t-s| \, \frac{I_N(M_1(t,s)\varphi(s)|X'(s)|)}{\sqrt{1-s^2}} + \frac{I_N(M_2(t,s)\varphi(s)|X'(s)|)}{\sqrt{1-s^2}} \, ds. \qquad (7.5)$$

First, $\mathcal{S}^0$ is a bounded operator, as stated in the next lemma (cf. [31]).

Lemma 7.2 *If $\varphi \in W_T^\sigma$, let*

$$\mathcal{S}^0\varphi = \int_{-1}^{1} \ln|t-s| \frac{\varphi(s)}{\sqrt{1-s^2}} \, ds,$$

then there exists a constant C such that

$$||\mathcal{S}^0\varphi||_\sigma \le C||\varphi||_\sigma.$$

The error estimate for $\mathcal{S}\varphi$ is given in the following theorem.

Theorem 7.2 *If $X(t) \in C^r[-1,1]$, $\varphi \in W_T^r[-1,1]$, and for any σ, $0 \le 2\sigma \le r$, then*

$$||\mathcal{S}\varphi - \mathcal{S}_N\varphi||_\sigma \le C\left(\frac{1}{N}\right)^{r-2\sigma} ||\varphi||_r.$$

Proof: From (7.4) and (7.5),

$$\begin{aligned}(\mathcal{S}-\mathcal{S}_N)\varphi &= \int_{-1}^{1} \ln|t-s| \left[M_1(t,s)\varphi(s)\frac{|X'(s)|}{\sqrt{1-s^2}} - \frac{I_N\left(M_1(t,s)\varphi(s)|X'(s)|\right)}{\sqrt{1-s^2}} \right] ds \\ &\quad + \int_{-1}^{1} M_2(t,s)\varphi(s)\frac{|X'(s)|}{\sqrt{1-s^2}} - \frac{I_N\left(M_2(t,s)\varphi(s)|X'(s)|\right)}{\sqrt{1-s^2}} \, ds \\ &=: A_1(t) + A_2(t).\end{aligned}$$

It is known that $M_1(t,s)$ and $M_2(t,s)$ are analytic functions. Therefore, by Lemma 7.1, $M_1(t,s)$ and $M_2(t,s)$ have the following expansions:

$$M_1(t,s) = \sum_{n=0}^{\infty} c_{n,1}(t)T_n(s), \qquad M_2(t,s) = \sum_{n=0}^{\infty} c_{n,2}(t)T_n(s). \qquad (7.6)$$

Next, we give the estimate of $||A_1(t)||_\sigma$ and $||A_2(t)||_\sigma$. By the expansion (7.6),

$$\begin{aligned}
||A_1(t)||_\sigma &= \Big|\Big| \sum_{n=0}^{\infty} c_{n,1}(t) \int_{-1}^{1} \ln|t-s| \left[T_n(s)\varphi(s) \frac{|X'(s)|}{\sqrt{1-s^2}} - \frac{I_N\left(T_n(s)\varphi(s)|X'(s)|\right)}{\sqrt{1-s^2}} \right] \Big|\Big|_\sigma \\
&\leq \sum_{n=0}^{\infty} \Big|\Big| c_{n,1}(t) \mathcal{S}^0 \left(T_n(s)\varphi(s)|X'(s)| - I_N(T_n(s)\varphi(s)|X'(s)|) \right) \Big|\Big|_\sigma \\
&\leq C \sum_{n=0}^{\infty} \Big|\Big| c_{n,1}(t) \Big|\Big|_{C^\sigma[-1,1]} \Big|\Big| \mathcal{S}^0 \left(T_n(s)\varphi(s)|X'(s)| - I_N(T_n(s)\varphi(s)|X'(s)|) \right) \Big|\Big|_\sigma .
\end{aligned}$$

By Lemma 7.2, Theorem 7.1 and the fact that $M_1(t,s)$ is an analytic function, it follows that

$$\begin{aligned}
||A_1(t)||_\sigma &\leq C \sum_{n=0}^{\infty} \Big|\Big| c_{n,1}(t) \Big|\Big|_{C^\sigma[-1,1]} \Big|\Big| T_n(s)\varphi(s)|X'(s)| - I_N(T_n(s)\varphi(s)|X'(s)|) \Big|\Big|_\sigma \\
&\leq C \sum_{n=0}^{\infty} \Big|\Big| c_{n,1}(t) \Big|\Big|_{C^\sigma[-1,1]} \left(\frac{1}{N} \right)^{r-2\sigma} \Big|\Big| T_n(s)\varphi(s)|X'(s)| \Big|\Big|_r \\
&\leq C \left(\frac{1}{N} \right)^{r-2\sigma} \sum_{n=0}^{\infty} \Big|\Big| c_{n,1}(t) \Big|\Big|_{C^\sigma[-1,1]} \Big|\Big| T_n(s) \Big|\Big|_{C^r[-1,1]} \Big|\Big| |X'(s)| \Big|\Big|_{C^r[-1,1]} ||\varphi||_r \\
&\leq C \left(\frac{1}{N} \right)^{r-2\sigma} \Big|\Big| \varphi \Big|\Big|_r . \qquad (7.7)
\end{aligned}$$

Next, we estimate $||A_2(t)||_\sigma$. By the expansion (7.6),

$$\begin{aligned}
A_2(t) &= \int_{-1}^{1} M_2(t,s)\varphi(s) \frac{|X'(s)|}{\sqrt{1-s^2}} - \frac{I_N\left(M_2(t,s)\varphi(s)|X'(s)|\right)}{\sqrt{1-s^2}}\, ds \\
&= \sum_{n=0}^{\infty} c_{n,2}(t) \int_{-1}^{1} T_n(s)\varphi(s) \frac{|X'(s)|}{\sqrt{1-s^2}} - \frac{I_N\left(T_n(s)\varphi(s)|X'(s)|\right)}{\sqrt{1-s^2}}\, ds.
\end{aligned}$$

Then,

$$\begin{aligned}
||A_2(t)||_\sigma &= \Big|\Big| \sum_{n=0}^{\infty} c_{n,2}(t) \int_{-1}^{1} T_n(s)\varphi(s) \frac{|X'(s)|}{\sqrt{1-s^2}} - \frac{I_N\left(T_n(s)\varphi(s)|X'(s)|\right)}{\sqrt{1-s^2}}\, ds \Big|\Big|_\sigma \\
&\leq C \left(\int_{-1}^{1} \left| T_n(s)\varphi(s) \frac{|X'(s)|}{\sqrt{1-s^2}} - \frac{I_N\left(T_n(s)\varphi(s)|X'(s)|\right)}{\sqrt{1-s^2}} \right| ds \right) \sum_{n=0}^{\infty} ||c_{n,2}(t)||_{c^\sigma[-1,1]} \\
&\leq C \int_{-1}^{1} \left| T_n(s)\varphi(s) \frac{|X'(s)|}{\sqrt{1-s^2}} - \frac{I_N\left(T_n(s)\varphi(s)|X'(s)|\right)}{\sqrt{1-s^2}} \right| ds \\
&= C \int_{-1}^{1} \left| T_n(s)\varphi(s)|X'(s)| - I_N(T_n(s)\varphi(s)|X'(s)|) \right| \frac{1}{\sqrt{1-s^2}}\, ds
\end{aligned}$$

$$= C\int_{-1}^{1}\Big|T_n(s)\varphi(s)|X'(s)| - I_N(T_n(s)\varphi(s)|X'(s)|)\Big|\left(\frac{1}{\sqrt{1-s^2}}\right)^{\frac{1}{2}}\left(\frac{1}{\sqrt{1-s^2}}\right)^{\frac{1}{2}}ds.$$

By the Holder inequality,

$$\begin{aligned}||A_2(t)||_\sigma &\leq C\left[\int_{-1}^{1}\frac{\Big|T_n(s)\varphi(s)|X'(s)| - I_N(T_n(s)\varphi(s)|X'(s)|)\Big|^2}{\sqrt{1-s^2}}ds\right]^{\frac{1}{2}}\left(\int_{-1}^{1}\frac{1}{\sqrt{1-s^2}}ds\right)^{\frac{1}{2}}\\ &\leq C\Big|\Big|T_n(s)\varphi(s)|X'(s)| - I_N(T_n(s)\varphi(s)|X'(s)|)\Big|\Big|_0.\end{aligned}$$

An application of Theorem 7.1 leads to

$$\begin{aligned}||A_2(t)||_\sigma &\leq C\Big|\Big|T_n(s)\varphi(s)|X'(s)| - I_N(T_n(s)\varphi(s)|X'(s)|)\Big|\Big|_0\\ &\leq C\left(\frac{1}{N}\right)^r\Big|\Big|T_n(s)\varphi(s)|X'(s)|\Big|\Big|_r\\ &\leq C\left(\frac{1}{N}\right)^r||\varphi(s)||_r\Big|\Big|T_n(s)\Big|\Big|_{C^r[-1,1]}\Big|\Big|X'(s)|\Big|\Big|_{C^r[-1,1]}\\ &\leq C\left(\frac{1}{N}\right)^r||\varphi(s)||_r\\ &\leq C\left(\frac{1}{N}\right)^{r-2\sigma}||\varphi(s)||_r. \qquad (7.8)\end{aligned}$$

Combining (7.7) and (7.8) yields

$$||\mathcal{S}\varphi - \mathcal{S}_N\varphi||_\sigma \leq C\left(\frac{1}{N}\right)^{r-2\sigma}||\varphi||_r. \qquad (7.9)$$

We remark that following the steps in Theorem 7.2, it is easy to obtain that

$$\begin{aligned}||\mathcal{S}\varphi||_r &\leq \Big|\Big|\int_{-1}^{1}\ln|t-s|M_1(t,s)\varphi(s)\frac{|X'(s)|}{\sqrt{1-s^2}}\,ds\Big|\Big|_r + \Big|\Big|\int_{-1}^{1}M_2(t,s)\varphi(s)\frac{|X'(s)|}{\sqrt{1-s^2}}\,ds\Big|\Big|_r\\ &\leq C\Big|\Big|T_n(s)\varphi(s)|X'(s)|\Big|\Big|_r + C\int_{-1}^{1}\Big|T_n(s)\varphi(s)\frac{|X'(s)|}{\sqrt{1-s^2}}\Big|\,ds\\ &\leq C\Big|\Big|T_n(s)\varphi(s)|X'(s)|\Big|\Big|_r + C\Big|\Big|T_n(s)\varphi(s)|X'(s)|\Big|\Big|_0\\ &\leq C\Big|\Big|T_n(s)\varphi(s)|X'(s)|\Big|\Big|_r \leq C||\varphi(s)||_r. \qquad (7.10)\end{aligned}$$

From the discussion in Section 4.2 and 4.3, the hypersingluar operator $\mathcal{T}$ can be decomposed as

$$\mathcal{T} = \mathcal{T}^g + \mathcal{T}^s,$$

as given by (4.28). Furthermore, $\mathcal{T}^s$ can be written as the composition of three operators

$$\mathcal{T}^s\phi = (\mathcal{T}_{1g} \cdot \mathcal{T}_{2g} \cdot \mathcal{T}_{3g})\,\phi.$$

where $\mathcal{T}_{1g}$, $\mathcal{T}_{2g}$ and $\mathcal{T}_{3g}$ are defined by (4.47), (4.48) and (4.49), respectively.

The next lemma gives bounds for the operators $\mathcal{T}_{1g}$, $\mathcal{T}_{2g}$ and $\mathcal{T}_{3g}$.

Lemma 7.3 *If $\varphi \in W_T^{r+1}[-1,1]$, then there exists constants such that*

$$||\mathcal{T}_{1g}\varphi||_r \le C||\varphi||_{r+1}, \quad ||\mathcal{T}_{2g}\varphi||_r \le C||\varphi||_r, \quad ||\mathcal{T}_{3g}\varphi||_r \le C||\varphi||_{r+1} \tag{7.11}$$

Remark: $\mathcal{T}_{1g}$ and $\mathcal{T}_{3g}$ are essentially the first-order differential operators, and their bounds are obvious. $\mathcal{T}_{2g}$ has the same kernel as $\mathcal{S}$, hence its bound follows from a similar proof as that of Theorem 7.2 .

We denote by $\mathcal{T}_{jg,N}$ ($j = 1, 2, 3$) the numerical approximation of $\mathcal{T}_{jg}$ by using Chebshev polynomials. Then their boundness is given in the following lemma.

Lemma 7.4 *If $\varphi \in W_T^{2(r+1)}[-1,1]$, then there exists constants such that*

$$||\mathcal{T}_{1g,N}\varphi||_r \le C||\varphi||_{2(r+1)}, \quad ||\mathcal{T}_{2g,N}\varphi||_r \le C||\varphi||_{2r}, \quad ||\mathcal{T}_{3g,N}\varphi||_r \le C||\varphi||_{2(r+1)}. \tag{7.12}$$

Proof: According to the definition of $\mathcal{T}_{1g}$ and the calculation of $\mathcal{T}_{1g,N}$, it follows that

$$\begin{aligned}
\mathcal{T}_{1g}\varphi &= \frac{1}{|X'(t)|}\left(-\frac{d\varphi}{dt}\right), \\
\mathcal{T}_{1g,N}\varphi &= \frac{1}{|X'(t)|}\left(-\frac{d(I_N(\varphi))}{dt}\right), \\
\mathcal{T}_{1g,N}\varphi &= (\mathcal{T}_{1g,N} - \mathcal{T}_{1g})\varphi + \mathcal{T}_{1g}\varphi.
\end{aligned}$$

From Theorem 7.1,

$$\begin{aligned}
\big|\big|(\mathcal{T}_{1g,N}-\mathcal{T}_{1g})\varphi\big|\big|_r &= \Big|\Big|\frac{1}{|X'(t)|}\left(\frac{d\varphi}{dt}-\frac{d(I_N(\varphi))}{dt}\right)\Big|\Big|_r \\
&\le C\Big|\Big|\frac{d\varphi}{dt}-\frac{d(I_N(\varphi))}{dt}\Big|\Big|_r \\
&\le C\big|\big|\varphi-I_N\varphi\big|\big|_{r+1} \\
&\le C||\varphi||_{2(r+1)}.
\end{aligned}$$

By Lemma 7.3,

$$||\mathcal{T}_{1g}\varphi||_r \le C||\varphi||_{r+1} \le C||\varphi||_{2(r+1)}.$$

Therefore,

$$\begin{aligned}
\big|\big|\mathcal{T}_{1g,N}\varphi\big|\big|_r &\le \big|\big|(\mathcal{T}_{1g,N}-\mathcal{T}_{1g})\varphi\big|\big|_r+\big|\big|\mathcal{T}_{1g}\varphi\big|\big|_r \\
&\le C||\varphi||_{2(r+1)}.
\end{aligned}$$

The estimate of $\mathcal{T}_{3g,N}$ can be obtained similarily.

For $\mathcal{T}_{2g,N}\varphi$,

$$\mathcal{T}_{2g,N}\varphi=(\mathcal{T}_{2g,N}-\mathcal{T}_{2g})\varphi+\mathcal{T}_{2g}\varphi.$$

By Lemma 7.3,

$$\big|\big|\mathcal{T}_{2g}\varphi\big|\big|_r \le C||\varphi||_r \le C||\varphi||_{2r}.$$

On the other hand, $(\mathcal{T}_{2g,N}-\mathcal{T}_{2g})\varphi$ has the same kernel as $(\mathcal{S}-\mathcal{S}_N)\varphi$, thus from Theorem 7.2, we obtain

$$\big|\big|(\mathcal{T}_{2g,N}-\mathcal{T}_{2g})\varphi\big|\big|_r \le C||\varphi||_{2r}.$$

Therefore,

$$\begin{aligned}
\big|\big|\mathcal{T}_{2g,N}\varphi\big|\big|_r &\le \big|\big|(\mathcal{T}_{2g,N}-\mathcal{T}_{2g})\varphi\big|\big|_r+\big|\big|\mathcal{T}_{2g}\varphi\big|\big|_r \\
&\le C||\varphi||_{2r}.
\end{aligned}$$

The next theorem gives an error estimate of the Nystrom discretization for $\mathcal{T}\varphi$.

Theorem 7.3 *If* $\varphi \in W_T^r(-1,1)$, $\frac{r}{4} - \frac{1}{2} - 2(\sigma+1) \geq 0$ *and* $\sigma \geq 0$, *then*

$$\left|\left|\mathcal{T}\varphi - \mathcal{T}_N\varphi\right|\right|_\sigma \leq C\left(\frac{1}{N}\right)^{\frac{r}{4}-\frac{1}{2}-2(\sigma+1)} ||\varphi||_r.$$

Proof: Since

$$\begin{aligned}\mathcal{T}\varphi &= \mathcal{T}^g\varphi + \mathcal{T}^s\varphi,\\ \mathcal{T}_N\varphi &= \mathcal{T}_N^g\varphi + \mathcal{T}_N^s\varphi.\end{aligned}$$

$\mathcal{T}^g\varphi$ has the same kernel as $\mathcal{S}$, then following the same proof in Theorem 7.2, we have

$$\left|\left|\mathcal{T}^g\varphi - \mathcal{T}_N^g\varphi\right|\right|_\sigma \leq Ck^2\left(\frac{1}{N}\right)^{r-2\sigma} ||\varphi||_r. \tag{7.13}$$

It is known that

$$\begin{aligned}\mathcal{T}^s &= \mathcal{T}_{1g}\mathcal{T}_{2g}\mathcal{T}_{3g},\\ \mathcal{T}_N^s &= \mathcal{T}_{1g,N}\cdot\mathcal{T}_{2g,N}\cdot\mathcal{T}_{3g,N}.\end{aligned}$$

$\mathcal{T}_{2g}\varphi$ has the same kernel as $\mathcal{S}$, then repeating the steps in the proof in Theorem 7.2 gives us

$$\left|\left|\mathcal{T}_{2g}\varphi - \mathcal{T}_{2g,N}\varphi\right|\right|_l \leq C\left(\frac{1}{N}\right)^{s-2l} ||\varphi||_s. \tag{7.14}$$

$\mathcal{T}_{1g}$ and $\mathcal{T}_{3g}$ are first-order differential operators. Therefore, from lemma 7.1,

$$\begin{aligned}\left|\left|(\mathcal{T}_{1g,N} - \mathcal{T}_{1g})\varphi\right|\right|_l &= \left|\left|\frac{1}{|X'(t)|}\left(\frac{d\varphi}{dt} - \frac{d(I_N(\varphi))}{dt}\right)\right|\right|_l\\ &\leq C\left|\left|\frac{d\varphi}{dt} - \frac{d(I_N(\varphi))}{dt}\right|\right|_l\\ &\leq C\left|\left|\varphi - I_N\varphi\right|\right|_{l+1}\\ &\leq C\left(\frac{1}{N}\right)^{s-2(l+1)} ||\varphi||_l \end{aligned}\tag{7.15}$$

Similarly, the following result holds:

$$\left|\left|(\mathcal{T}_{3g,N} - \mathcal{T}_{3g})\varphi\right|\right|_l \leq C\left(\frac{1}{N}\right)^{s-2(l+1)} ||\varphi||_l \tag{7.16}$$

To estimate $\left|\left|\mathcal{T}_{1g}\mathcal{T}_{2g}\mathcal{T}_{3g}\varphi - \mathcal{T}_{1g,N}\mathcal{T}_{2g,N}\mathcal{T}_{3g,N}\varphi\right|\right|_\sigma$, we split the difference as follows:

$$\begin{aligned}\mathcal{T}_{1g}\mathcal{T}_{2g}\mathcal{T}_{3g}\varphi - \mathcal{T}_{1g,N}\mathcal{T}_{2g,N}\mathcal{T}_{3g,N}\varphi &= (\mathcal{T}_{1g}\mathcal{T}_{2g}\mathcal{T}_{3g}\varphi - \mathcal{T}_{1g}\mathcal{T}_{2g}\mathcal{T}_{3g,N}\varphi) \\ &+ (\mathcal{T}_{1g}\mathcal{T}_{2g}\mathcal{T}_{3g,N}\varphi - \mathcal{T}_{1g}\mathcal{T}_{2g,N}\mathcal{T}_{3g,N}\varphi) \\ &+ (\mathcal{T}_{1g}\mathcal{T}_{2g,N}\mathcal{T}_{3g,N}\varphi - \mathcal{T}_{1g,N}\mathcal{T}_{2g,N}\mathcal{T}_{3g,N}\varphi) \end{aligned} \tag{7.17}$$

From lemma 7.3 and (7.16),

$$\begin{aligned}\left|\left|\mathcal{T}_{1g}\mathcal{T}_{2g}\mathcal{T}_{3g}\varphi - \mathcal{T}_{1g}\mathcal{T}_{2g}\mathcal{T}_{3g,N}\varphi\right|\right|_\sigma &\leq C\left|\left|\mathcal{T}_{3g}\varphi - \mathcal{T}_{3g,N}\varphi\right|\right|_{\sigma+1} \\ &\leq C\left(\frac{1}{N}\right)^{r-2(\sigma+1)} ||\varphi||_r. \end{aligned} \tag{7.18}$$

From lemma 7.3, (7.14) and lemma 7.4,

$$\begin{aligned}\left|\left|\mathcal{T}_{1g}\mathcal{T}_{2g}\mathcal{T}_{3g,N}\varphi - \mathcal{T}_{1g}\mathcal{T}_{2g,N}\mathcal{T}_{3g,N}\varphi\right|\right|_\sigma &\leq C\left|\left|\mathcal{T}_{2g}\mathcal{T}_{3g,N}\varphi - \mathcal{T}_{2g,N}\mathcal{T}_{3g,N}\varphi\right|\right|_{\sigma+1} \\ &\leq C\left(\frac{1}{N}\right)^{\frac{r}{2}-1-2(\sigma+1)} ||\mathcal{T}_{3g,N}\varphi||_{\frac{r}{2}-1} \\ &\leq C\left(\frac{1}{N}\right)^{\frac{r}{2}-1-2(\sigma+1)} ||\varphi||_r. \end{aligned} \tag{7.19}$$

From (7.15) and lemma 7.4 ,

$$\begin{aligned}\left|\left|\mathcal{T}_{1g}\mathcal{T}_{2g,N}\mathcal{T}_{3g,N}\varphi - \mathcal{T}_{1g,N}\mathcal{T}_{2g,N}\mathcal{T}_{3g,N}\varphi\right|\right|_\sigma &\leq C\left(\frac{1}{N}\right)^{\frac{r}{4}-\frac{1}{2}-2(\sigma+1)} \left|\left|\mathcal{T}_{2g,N}\mathcal{T}_{3g,N}\varphi\right|\right|_{\frac{r}{4}-\frac{1}{2}} \\ &\leq C\left(\frac{1}{N}\right)^{\frac{r}{4}-\frac{1}{2}-2(\sigma+1)} \left|\left|\mathcal{T}_{3g,N}\varphi\right|\right|_{\frac{r}{2}-1} \\ &\leq C\left(\frac{1}{N}\right)^{\frac{r}{4}-\frac{1}{2}-2(\sigma+1)} ||\varphi||_r. \end{aligned} \tag{7.20}$$

From (7.18), (7.19) and (7.20),

$$\left|\left|\mathcal{T}_{1g}\mathcal{T}_{2g}\mathcal{T}_{3g}\varphi - \mathcal{T}_{1g,N}\mathcal{T}_{2g,N}\mathcal{T}_{3g,N}\varphi\right|\right|_{\sigma} \leq C\left(\frac{1}{N}\right)^{\frac{r}{4}-\frac{1}{2}-2(\sigma+1)} ||\varphi||_r. \tag{7.21}$$

From (7.13) and (7.21), we have

$$||\mathcal{T}\varphi - \mathcal{T}_N\varphi||_{\sigma} \leq C\left(\frac{1}{N}\right)^{\frac{r}{4}-\frac{1}{2}-2(\sigma+1)} ||\varphi||_r.$$

7.3 Error estimation for the solution of the boundary integral equation

In this section, we employ the results obtained in the last section to derive an error estimate for $\mathcal{A}$ and the solution of the boundary integral equation.

In our boundary integral equation formulation,

$$\mathcal{A}\varphi = \left(\sqrt{1-t^2}\mathcal{S} - \frac{i\tau}{k}\mathcal{T}\mathcal{S}\right)\varphi.$$

We denote the numerical evaluation of $\mathcal{A}$ by $\mathcal{A}_N$.

Theorem 7.4 *If $\varphi \in W_T^r[-1,1]$ and $r \geq 20$, then*

$$\left|\left|\mathcal{A}\varphi - \mathcal{A}_N\varphi\right|\right|_0 \leq C\left(\frac{1}{N}\right)^{\frac{r}{8}-\frac{5}{2}} ||\varphi||_r.$$

Proof: Since

$$\mathcal{A}\varphi - \mathcal{A}_N\varphi = \sqrt{1-t^2}(\mathcal{S}\varphi - \mathcal{S}_N\varphi) - \frac{i\tau}{k}(\mathcal{T}\mathcal{S}\varphi - \mathcal{T}_N\mathcal{S}_N\varphi).$$

From Theorem 7.2,

$$\begin{aligned}\left|\left|\sqrt{1-t^2}(\mathcal{S}\varphi - \mathcal{S}_N\varphi)\right|\right|_0 &\leq C\left|\left|\mathcal{S}\varphi - \mathcal{S}_N\varphi\right|\right|_0 \\ &\leq C\left(\frac{1}{N}\right)^{r} ||\varphi||_r. \end{aligned} \tag{7.22}$$

And

$$\mathcal{T}\mathcal{S}\varphi - \mathcal{T}_N\mathcal{S}_N\varphi = (\mathcal{T}\mathcal{S}\varphi - \mathcal{T}\mathcal{S}_N\varphi) + (\mathcal{T}\mathcal{S}_N\varphi - \mathcal{T}_N\mathcal{S}_N\varphi).$$

From Lemma 7.3 and Theorem 7.2,

$$\begin{aligned} \left|\left|\mathcal{T}\mathcal{S}\varphi - \mathcal{T}\mathcal{S}_N\varphi\right|\right|_0 &\leq C\left|\left|\mathcal{S}\varphi - \mathcal{S}_N\varphi\right|\right|_2 \\ &\leq C\left(\frac{1}{N}\right)^{r-4}||\varphi||_r. \end{aligned} \tag{7.23}$$

From Theorem 7.2 and (7.10),

$$\begin{aligned} ||\mathcal{S}_N\varphi||_\sigma &\leq \left|\left|\mathcal{S}\varphi - \mathcal{S}_N\varphi\right|\right|_\sigma + \left|\left|\mathcal{S}\varphi\right|\right|_\sigma \\ &\leq C||\varphi||_{2\sigma} + C||\varphi||_\sigma \\ &\leq C||\varphi||_{2\sigma}. \end{aligned} \tag{7.24}$$

By Theorem 7.3 and (7.24),

$$\begin{aligned} \left|\left|\mathcal{T}\mathcal{S}_N\varphi - \mathcal{T}_N\mathcal{S}_N\varphi\right|\right|_0 &\leq C\left(\frac{1}{N}\right)^{\frac{r}{8}-\frac{5}{2}}||\mathcal{S}_N\varphi||_{\frac{r}{2}} \\ &\leq C\left(\frac{1}{N}\right)^{\frac{r}{8}-\frac{5}{2}}||\varphi||_r. \end{aligned} \tag{7.25}$$

From (7.23) and (7.25), we have

$$\left|\left|\mathcal{T}\mathcal{S}\varphi - \mathcal{T}_N\mathcal{S}_N\varphi\right|\right|_0 \leq C\left(\frac{1}{N}\right)^{\frac{r}{8}-\frac{5}{2}}||\varphi||_r. \tag{7.26}$$

Therefore, by (7.22) and (7.26), we finally get that

$$\begin{aligned} \left|\left|\mathcal{A}\varphi - \mathcal{A}_N\varphi\right|\right|_0 &\leq C\left(\frac{1}{N}\right)^r||\varphi||_r + C\left(\frac{1}{N}\right)^{\frac{r}{8}-\frac{5}{2}}||\varphi||_r \\ &\leq C\left(\frac{1}{N}\right)^{\frac{r}{8}-\frac{5}{2}}||\varphi||_r. \end{aligned}$$

The formulation in our problem

$$\mathcal{A}\varphi = h$$

has a discretized version in which we look to solve for φ_N from

$$\mathcal{A}_N \varphi_N = h.$$

Theorem 7.5 *If $\varphi \in W_T^r[-1,1]$ and $r \geq 20$, then*

$$\left|\left|\varphi - \varphi_N\right|\right|_0 \leq C \left(\frac{1}{N}\right)^{\frac{r}{8}-\frac{5}{2}} ||\varphi||_r. \tag{7.27}$$

Proof: $\mathcal{A}\varphi - \mathcal{A}_N\varphi_N = 0$ leads to

$$(\mathcal{A}\varphi - \mathcal{A}_N\varphi) + (\mathcal{A}_N\varphi - \mathcal{A}_N\varphi_N) = 0.$$

Thus,

$$\mathcal{A}_N(\varphi - \varphi_N) = -(\mathcal{A}\varphi - \mathcal{A}_N\varphi).$$

From Theorem 7.4, since

$$\left|\left|\mathcal{A}\varphi - \mathcal{A}_N\varphi\right|\right|_0 \leq C \left(\frac{1}{N}\right)^{\frac{r}{8}-\frac{5}{2}} ||\varphi||_r,$$

we finally arrive at

$$\begin{aligned} \left|\left|\varphi - \varphi_N\right|\right|_0 &\leq C\left|\left|\mathcal{A}\varphi - \mathcal{A}_N\varphi\right|\right|_0 \\ &\leq C \left(\frac{1}{N}\right)^{\frac{r}{8}-\frac{5}{2}} ||\varphi||_r. \end{aligned} \tag{7.28}$$

This completes the error estimation for the solution φ to the boundary integral equation

$$\mathcal{A}\varphi = h.$$

References

[1] F. Javier Garca de Abajo, “Colloquium: Light scattering by particle and hole arrays.” Reviews of Modern Physics, no. 79 (2007):1267.

[2] F. Javier Garca de Abajo, “Graphene plasmonics: challenges and opportunities.” Acs Photonics 1, no. 3 (2014): 135-152.

[3] Robert A. Adams and John JF Fournier, “Sobolev spaces.” Vol. 140. Academic press, 2003.

[4] Kendall E. Atkinson and Ian H. Sloan, “The numerical solution of first-kind logarithmic-kernel integral equations on smooth open arcs.” Mathematics of Computation 56, no. 193 (1991): 119-139.

[5] W. Barnes, A. Dereux, and T. Ebbesen, ”Surface plasmon subwavelength optics”, Nature 424, no. 6950 (2003): 824.

[6] Yu. V. Bludov, Aires Ferreira, N. M. R. Peres and M. I. Vasilevskiy, “A primer on surface plasmon-polaritons in graphene.” International Journal of Modern Physics B 27, no. 10 (2013): 1341001.

[7] Carlos Alberto Brebbia and Stephen Walker, “Boundary element techniques in engineering.” Elsevier, 2016.

[8] Oscar P. Bruno and Stephane K. Lintner, “Second-kind integral solvers for TE and TM problems of diffraction by open arcs.” Radio Science 47, no. 6 (2012).

[9] Oscar P. Bruno and Michael C. Haslam. "Regularity theory and superalgebraic solvers for wire antenna problems." SIAM Journal on Scientific Computing 29.4 (2007): 1375-1402.

[10] Claudio Canuto and Alfio Quarteroni, "Approximation results for orthogonal polynomials in Sobolev spaces." Mathematics of Computation 38, no. 157 (1982): 67-86.

[11] Jierong Cheng, Wei Li Wang, Hossein Mosallaei and Efthimios Kaxiras, "Surface plasmon engineering in graphene functionalized with organic molecules: a multiscale theoretical investigation." Nano letters 14, no. 1 (2013): 50-56.

[12] S. H. Christiansen and J. C. Nedelec, "Preconditioners for the boundary element method in acoustics." Mathematical and numerical aspects of wave propagation (Santiago de Compostela, 2000) (2000): 776-781.

[13] David Colton and Rainer Kress, "Inverse acoustic and electromagnetic scattering theory." Vol. 93. Springer Science & Business Media, 2012.

[14] David Colton and Rainer Kress, "Integral equation methods in scattering theory." Vol. 72. SIAM, 2013.

[15] Thomas W. Ebbesen, H. J. Lezec, H. F. Ghaemi, Tineke Thio and P. A. Wolff, "Extraordinary optical transmission through sub-wavelength hole arrays." Nature 391, no. 6668 (1998): 667.

[16] Ugo Fano, "Some theoretical considerations on anomalous diffraction gratings." Physical Review 50, no. 6 (1936): 573.

[17] Ugo Fano, "On the anomalous diffraction gratings. II." Physical Review 51, no. 4 (1937): 288.

[18] Juan Luis Garcia-Pomar, Alexey Yu. Nikitin and Luis Martin-Moreno, "Scattering of graphene plasmons by defects in the graphene sheet." ACS nano 7, no. 6 (2013): 4988-4994.

[19] Martin A. Green and Supriya Pillai, "Harnessing plasmonics for solar cells." Nature Photonics 6, no. 3 (2012): 130.

[20] A. N. Grigorenko, Marco Polini and K. S. Novoselov, "Graphene plasmonics." Nature photonics 6, no. 11 (2012): 749.

[21] George C. Hsiao, Ernst P. Stephan and Wolfgang L. Wendland, "On the Dirichlet problem in elasticity for a domain exterior to an arc." Journal of computational and applied mathematics 34, no. 1 (1991): 1-19.

[22] George C. Hsiao and Wolfgang L. Wendland, "Boundary integral equations." Springer Berlin Heidelberg, 2008.

[23] J. David Jackson, "Electrodynamics." Wiley-VCH Verlag GmbH & Co. KGaA, 1975.

[24] Shidong Jiang and Vladimir Rokhlin, "Second kind integral equations for the classical potential theory on open surfaces II." Journal of Computational Physics 195, no. 1 (2004): 1-16.

[25] Long Ju, Baisong Geng, Jason Horng, Caglar Girit, Michael Martin, Zhao Hao, Hans A. Bechtel et al, "Graphene plasmonics for tunable terahertz metamaterials." Nature nanotechnology 6, no. 10 (2011): 630.

[26] Andreas Kirsch and Peter Monk, "An analysis of the coupling of finite-element and Nystrom methods in acoustic scattering." IMA Journal of numerical analysis 14, no. 4 (1994): 523-544.

[27] Katrin Kneipp, Martin Moskovits and H. Kneipp, "Surface-enhanced Raman scattering." Physics Today 60, no. 11 (2007): 40.

[28] Frank H.L. Koppens, Darrick E. Chang and F. Javier Garcia de Abajo, "Graphene plasmonics: a platform for strong light-matter interactions." Nano letters 11, no. 8 (2011): 3370-3377.

[29] Rainer Kress, “A Nystrom method for boundary integral equations in domains with corners.” Numerische Mathematik 58, no. 1 (1990): 145-161.

[30] Rainer Kress, “Boundary integral equations in time-harmonic acoustic scattering.” Mathematical and Computer Modeling 15, no. 3-5 (1991): 229-243.

[31] Rainer Kress, “Linear integral equations.” Vol. 82 of Applied Mathematical Sciences. 1999.

[32] Rainer Kress, “On the numerical solution of a hypersingular integral equation in scattering theory.” Journal of computational and applied mathematics 61, no. 3 (1995): 345-360.

[33] Stephane K. Lintner and Oscar Bruno. ”A generalized Calderon formula for open-arc diffraction problems: theoretical considerations.” Proceedings of the Royal Society of Edinburgh Section A: Mathematics 145.2 (2015): 331-364.

[34] Tony Low, “2D materials polaritonics-quick tutorial.” Presentation, IMA, University of Minnesota, 6-10th Feb 2017.

[35] Tony Low and Phaedon Avouris, “Graphene plasmonics for terahertz to mid-infrared applications.” ACS nano 8, no. 2 (2014): 1086-1101.

[36] Matthias Maier, Dionisios Margetis and Mitchell Luskin, “Dipole excitation of surface plasmon on a conducting sheet: Finite element approximation and validation.” Journal of Computational Physics 339 (2017): 126-145.

[37] Matthias Maier, Dionisios Margetis and Mitchell Luskin, “Generation of surface plasmon-polaritons by edge effects.” arXiv preprint arXiv:1702.00848 (2017).

[38] Matthias Maier, Dionisios Margetis and Mitchell Luskin, “Finite element simulation of surface plasmon polaritons on 2D materials.” Presentation, IMA seminar, Mar 2017.

[39] Stefan Alexander Maier,“ Plasmonics: fundamentals and applications.” Springer Science & Business Media, 2007.

[40] Dionisios Margetis and Mitchell Luskin, “On solutions of Maxwell’s equations with dipole sources over a thin conducting film.” Journal of Mathematical Physics 57, no. 4 (2016): 042903.

[41] Dionisios Margetis, Matthias Maier and Mitchell Luskin, “On the Wiener-Hopf Method for Surface Plasmons: Diffraction from Semiinfinite Metamaterial Sheet.” Studies in Applied Mathematics 139, no. 4 (2017): 599-625.

[42] Luis Martin-Moreno, F. J. Garcia-Vidal, H. J. Lezec, K. M. Pellerin, Tineke Thio, J. B. Pendry and T. W. Ebbesen, “Theory of extraordinary optical transmission through subwavelength hole arrays.” Physical Review Letters 86, no. 6 (2001): 1114.

[43] John. C. Mason and David C. Handscomb, ”Chebyshev polynomials.” CRC Press, 2002.

[44] David Nicholls, ”Numerical Simulation of Grating Structures Incorporating Two-Dimensional Materials: A High-Order Perturbation of Surfaces Framework.” SIAM Journal on Applied Mathematics 78.1 (2018): 19-44.

[45] Lars Monch, “On the numerical solution of the direct scattering problem for an open sound-hard arc.” Journal of Computational and Applied mathematics 71, no. 2 (1996): 343-356.

[46] Jean-Claude Nedelec, “Acoustic and electromagnetic equations.” Vol.144 of Applied Mathematical Sciences. 2001.

[47] Alexey Yu. Nikitin, F. Guinea, F. J. Garca-Vidal and Luis Martn-Moreno, “Edge and waveguide terahertz surface plasmon modes in graphene microribbons.” Physical Review B 84, no. 16 (2011): 161407.

[48] William H. Press, “Numerical recipes 3rd edition: The art of scientific computing. ” Cambridge university press, 2007.

[49] Lord Rayleigh, “III. Note on the remarkable case of diffraction spectra described by Prof. Wood.” The London, Edinburgh, and Dublin Philosophical Magazine and Journal of Science 14, no. 79 (1907): 60-65.

[50] T. M. Slipchenko, M. L. Nesterov, Luis Martin-Moreno and Alexey Yu. Nikitin, “Analytical solution for the diffraction of an electromagnetic wave by a graphene grating.” Journal of Optics 15, no. 11 (2013): 114008.

[51] Ernst P. Stephan and Thanh Tran, “Domain decomposition algorithms for indefinite hypersingular integral equations: the h and p versions.” SIAM Journal on Scientific Computing 19, no. 4 (1998): 1139-1153.

[52] Ernst P. Stephan and Wolfgang L. Wendland, “An augmented Galerkin procedure for the boundary integral method applied to two-dimensional screen and crack problems.” Applicable Analysis 18, no. 3 (1984): 183-219.

[53] Eitan Tadmor, “The exponential accuracy of Fourier and Chebyshev differencing methods.” SIAM Journal on Numerical Analysis 23, no. 1 (1986): 1-10.

[54] Lloyd N. Trefethen and David Bau III, “Numerical linear algebra. ” Vol. 50. Siam, 1997.

[55] W. L. Wendland and E. P. Stephan, “A hypersingular boundary integral method for two-dimensional screen and crack problems.” Archive for Rational Mechanics and Analysis 112, no. 4 (1990): 363-390.

[56] Katherine A. Willets and Richard P. Van Duyne, ”Localized surface plasmon resonance spectroscopy and sensing.” Annu. Rev. Phys. Chem. 58 (2007): 267-297.

[57] Robert Williams Wood, “XLII. On a remarkable case of uneven distribution of light in a diffraction grating spectrum.” The London, Edinburgh, and Dublin Philosophical Magazine and Journal of Science 4, no. 21 (1902): 396-402.

[58] Hugen Yan, Tony Low, Wenjuan Zhu, Yanqing Wu, Marcus Freitag, Xuesong Li, Francisco Guinea, Phaedon Avouris and Fengnian Xia, “Damping pathways of mid-infrared plasmons in graphene nanostructures.” Nature Photonics 7, no. 5 (2013): 394.